Chemical and Process Engineering: New Frontiers, 2023, 44(1), e5
DOI: 10.24425/cpe.2023.142294

Mercury capture in process gases and its mechanisms in different industries: theoretical and practical aspects, including the influence of sulfur compounds on mercury removal

Yinyou Deng[1]*, Mariusz Macherzyński[2]

[1] AGH Doctoral School, AGH University of Science and Technology, Mickiewicza 30, 30-059 Krakow, Poland
[2] AGH University of Science and Technology, Department of Coal Chemistry and Environmental Sciences, Faculty of Fuel and Energy, Mickiewicza 30, 30-059, Krakow, Poland

*** Corresponding author:**
e-mail:
yinyoudeng@gmail.com

Article info:
Received: 05 September 2022
Revised: 17 February 2023
Accepted: 24 March 2023

Abstract
Mercury is a highly toxic metal which naturally occurs in the Earth's crust and has adverse effects on both humans and the environment. The use of fossil fuels for electricity generation and specific industries sources of mercury emissions. These emissions depend on the mercury content in fuels of different types, the process gas temperature and composition, the implementation of air pollutant control devices (APCDs), etc. The APCDs partially capture and/or oxidize mercury in flue gas as a side benefit. In some cases, the emissions are reduced by mercury-dedicated or mixed methods. Mercury transformation in process gases is generally based on a chain of homogeneous and/or heterogeneous reactions. The theory of gaseous mercury/solid phase reactions and its mechanisms is widely studied in the literature. In this review, we focused on the theoretical and practical studies of these mechanisms, including mercury oxidization and capture from specified laboratory simulated or process gases and industries. We summarized research on various reactions – mostly of a chemical type – between different forms of mercury derived from process gases, and solids, including particles of different kinds (fly ash, adsorbents or catalysts). We additionally reviewed the literature on the interactions between mercury and sulfur compounds in the simulated and process gases.

Keywords
mercury, process gas, mercury capture, mercury oxidation, industrial emissions

1. INTRODUCTION

Humans have been using mercury and mercuric products for over 3000 years, for example in pigments, anti-rot paints, and in some drugs. In the 20th century, mercury began to be used for electronic devices like batteries, thermometers, barometers, and manometers, in whitening cosmetics, and in dental amalgams. The United Nations Environment Programme (UNEP) has indicated that the ocean is the primary source of mercury emissions (UN Environment, 2019). Around 2900–4000 tonnes of mercury are re-emitted from the ocean annually. Two-thirds of mercury emissions from the ocean originate from anthropogenic activities, which have been contributing to oceanic mercury levels since the 16th century. Most anthropogenic mercury inputs are a result of gold and silver mining, fossil fuel combustion and industrial production (Table 1). Moreover, mercury can be transported over long distances, is persistent, and can bioaccumulate in biological chains. It has no recognized positive activity in biological systems.

Mercury ions, especially at high concentrations, tend to increase the formation of reactive oxygen species (ROS) such as superoxide oxygen (O^{2-}), hydroxyl radical (OH^{-}), and hydrogen peroxide (H_2O_2) (Gallego et al., 2002). A physiological process usually produces ROS at low concentrations, and they are vital for cell signaling, but when ROS are present in cells at higher concentrations, they have an adverse effect on cell structures and cell components (Ferreira et al., 2018). The US Poison Center has reported that 15,552 Americans were exposed to elemental mercury between 2001 and 2005. In 91% of these cases, the exposure was unintentional (Caravati et al., 2008). It was reported that cement production, gold mining, and fossil fuel energy generation were the primary sources of anthropogenic mercury emissions (UN Environment, 2019). The greatest single anthropogenic source of mercury emissions is artisanal and small-scale gold mining (ASGM), which contributed 838 tonnes of mercury into the atmosphere in 2015, accounting for 37.7% of total mercury emissions in that year. The second and third greatest sources of mercury emission are stationary fossil fuel combustion power plants (294.8 tonnes) and cement production (233 tonnes), accounting for 13.23% and 10.5% of total mercury emissions respectively (Table 1). Some gaseous fuels are also high in mercury (Kho et al., 2022; Mojammal et al., 2019).

The international community is making efforts to reduce definitely fossil fuel use over the next forty, fifty years, for example through implementation of renewable energy sources, de-

Table 1. Quantities of mercury emitted to air from anthropogenic sources in 2015, by different sectors (UN Environment, 2019).

Sectors	Mercury emission(tonne)	Percentage of total emission (%)
Artisanal and small-scale gold mining (ASGM)	838	37.7
Biomass burning (domestic, industrial and power plant)	51.9	2.33
Cement production (raw materials and fuel, excluding coal)	233	10.5
Cremation emissions	3.77	0.17
Chlor-alkali production (mercury process)	15.1	0.68
Non-ferrous metal production (primary Al, Cu, Pb, Zn)	228	10.3
Large-scale gold production	84.5	3.8
Mercury production	13.8	0.62
Oil refining	14.4	0.65
Pig iron and steel production (primary)	29.8	1.34
Stationary combustion of fossil fuel (domestic/residential, transportation)	58.7	2.64
Stationary combustion of fossil fuel (industrial)	127.5	5.74
Stationary combustion of fossil fuel (power plants)	294.8	13.23
Secondary steel production	10.1	0.46
Vinyl-chloride monomer (mercury catalyst)	58.2	2.6
Waste (other waste)	147	6.6
Waste incineration (controlled burning)	15.0	0.67
Total	2220	100

carbonization, sustainable development, zero emission techniques and circular economics. Nevertheless, some developing countries, specific industries, waste utilization technologies and small, but scattered heat producers, will still be using conventional fossil fuels in the future, and will be emitting mercury. Therefore, the well-defined knowledge about mercury capture methods from process gases is needed. The passive methods occur with other technologies cleaning exhaust gases, to distinguish with dedicated methods, designed only to remove mercury (methods of active and/or specific mechanisms of its removal), and mixed methods, where mercury is only one of several components that are to be captured from process gases (Macherzynski, 2018). In this review, the up-to-date status on the theoretical and practical studies on the mechanisms of capture from different process gases and industries was presented.

2. METHODS FOR REMOVAL OF MERCURY FROM PROCES GASES

2.1. The chemistry of mercury and its controls in the combustion of solids

Elemental mercury (Hg(0)) vapors cannot easily be removed from any process gases in industrial installations by conventional techniques (such as by exploiting low chemical activity or volatility), and these gases are thus considered to be the main source of anthropogenic mercury in the atmosphere. The use of dedicated catalysts and sorbents may be sufficient to control mercury and other gas pollutants in process gases of certain specific origins. Usually Hg(0) is adsorbed and oxidized to Hg^{2+} by catalysts as well as by Cl_2, O_2, and NO_x. This process may also occur at the surface of adsorbents. The processes discussed in this section may apply to coal-fired boilers of different kinds and installations for the incineration of municipal wastes, special wastes, and sludge.

Many researchers have investigated mercury transformation mechanisms and demonstrated its speciation in flue gas by air pollution control systems (Hall et al., 1991; Qiao et al., 2007). Mercury occurs in coal and can start to volatilize from the fuel at temperatures of around 150 °C. The volatilization rate of total Hg in the Argonne Premium Coal Samples is about 40%–75% at 550 °C (Finkelman et al., 1990; Uruski et al., 2015). When the temperature is higher than 800 °C, most of Hg is released from mercury compounds and volatilized. Table 2 showed the temperature at which different kinds of mercury compounds undergo decomposition and evaporation.

On the other hand, inside coal-fired boilers, at temperatures higher than 1000 °C, all mercury compounds are decomposed

Table 2. Thermal decomposition and evaporation temperature of mercury and its most important compounds.

Mercury compounds	Process	Peak range [°C]	Peak temp. [°C]	Source
Hg(0)	Boils		356; 357.3	Merdes et al. (1998); Zulaikhah et al. (2020)
Hg_2Cl_2	Sublimation		400	Gołaś and Strugała (2013)
	Thermal decomposition	30–370; 60–250	119; 138; 228	Sui et al. (2015); Zhang et al. (2019)
$HgCl_2$	Boils		302	Merdes et al. (1998); Li et al. (2022a)
	Thermal decomposition	70–220; 50–600	120; 249	Cao et al. (2020b); Sui et al. (2015)
HgS	Sublimation		583.5	Merdes et al. (1998)
	Thermal decomposition	170–290 (black); 240–350 (red)	245 (black); 310 (red); 400	Luo et al. (2011); Cao et al. (2020a)
HgO	Thermal decomposition	350–480; 190–530	430	Uruski et al. (2015); Cao et al. (2020b)
$HgSO_4$	Thermal decomposition	220–450; 500–600	390; 580	Rumayor et al. (2015); Uruski et al. (2015); Cao et al. (2020b)
Hg_2SO_4	Thermal decomposition	200–400; 410–600	225; 359; 560	Liu et al. (2013); Sui et al. (2015); Rumayor et al. (2015)
Pyrite-bound Hg	Thermal decomposition	180–300 (Pyrite I) 520–600 (Pyrite II)	251 (Pyrite I) 325; 551 (Pyrite II)	Merdes et al. (1998); Cao et al. (2020a)

into Hg(0) (Galbreath et al., 2000). Hg(0) is the only thermodynamically stable species above 750 °C (Li et al., 2022a; Pavlish et al., 2003; Senior et al., 2000a). Hg(0) oxidation starts at temperatures below 700 °C, and mercury is partially oxidized at (or below) 450 °C (Li et al., 2022a; Senior et al., 2000a). When mercury vapors cool off, they undergo numerous homogenous and/or heterogeneous reactions with other gases and fly ash components. In process gases cooled down to around 400 °C, Hg(0) is partially oxidized, through gas phase reactions involving oxygen and halogen species (Cl^- or Br^-), into Hg^{1+} and Hg^{2+}. Hg^{1+} is continuously oxidized into Hg^{2+} in a post-combustion step. $HgCl_2$ and HgO(g) are stable mercury species in flue gas at temperatures lower than 400 °C, but $HgCl_2$ is dominant in process gases containing chlorine (Pavlish et al., 2003). Finally, mercury may be emitted to the environment as Hg(0), oxidized mercury $Hg^{2+}X$ (X represents Cl_2, O, SO_4, S, etc.) (Fig. 1) or as the particulate-bound mercury Hg(p) (Gibb et al., 2000; Qiao et al., 2007;

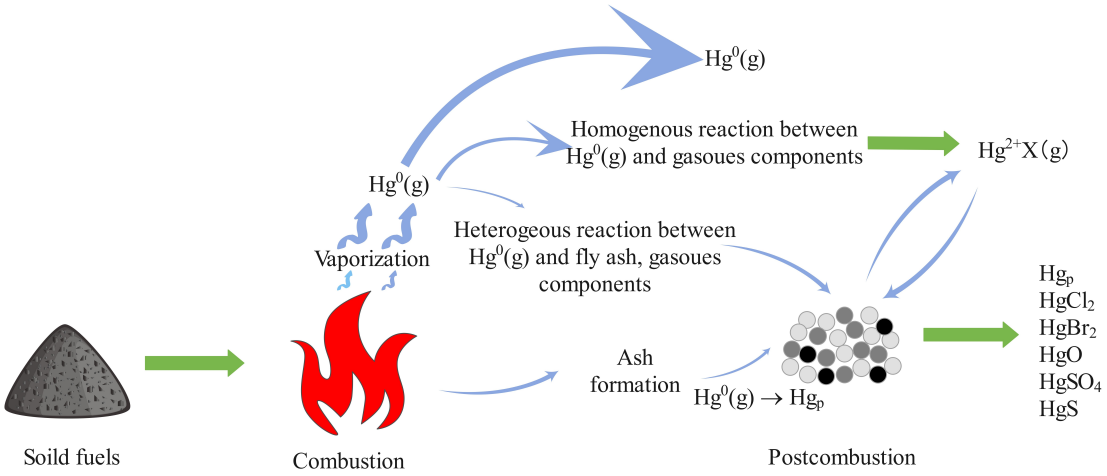

Figure 1. Transformations of mercury in solid combustion processes and flue gas (Galbreath et al., 2000).

Wang et al., 2009). Elemental mercury is the prevalent Hg species (82%) in flue gas, with lower proportions of Hg^{2+} (18%) (Font et al., 2012). In specific situations, dissolved mercury may occur in condensates or wastewater. The oxidized forms of mercury easily bind to fly ash or gypsum, which has a very positive effect on the emitted Hg(0) load.

Many factors affect the concentrations of mercury in flue gas and its removal, including coal type, flue gas components, the specific mercury species in the flue gas, fly ash composition, and operating conditions. The catalysts or adsorbents used in active mercury removal methods are also important. Mercury content in coal (Table 3) varies across coal basins, and according to geological factors such as depositional environment, and different coal-forming periods, as well as different degrees of deterioration. The use of inappropriate coal as an energy source can result in high mercury emissions in the exhaust gas.

Table 3. Mercury content in selected coals.

Country	Mercury content (μg/kg)	Source
China	134.33–231.03	Liu et al. (2019)
	124.84–647.42	Zhao et al. (2019b)
	112.1–292.6	Su et al. (2021)
	78–393	Ren et al. (2021)
	73–319	Huang et al. (2022)
India	110–800	Mukherjee et al. (2008)
	120–1080	Raj et al. (2017)
Russia	20–900	Mukherjee et al. (2008)
	10–2930	Osipova et al. (2019)
US	0–10000	Finkelman (1993)
	17.1–81.9	Gingerich et al. (2019)
UK	12–600	Białecka and Pyka (2016)
South Africa	140–300	Zhao et al. (2019a)
	10–493	Mathebula et al. (2020)
Poland	52–125	Wierzchowski et al. (2017)
	22–445	Auguścik-Górajek and Nieć (2020)
	63–139	Dziok et al. (2020)
	67.8–276	Okońska et al. (2013)
	1–758	Michalska et al. (2022)
	13–163	Białecka and Pyka (2016)
Australia	10–140	Zhao et al. (2019a)
	40.3–46.5	Schneider et al. (2021)
World	20–1000	Kolker et al. (2006)
	100 (mean)	Senior et al. (2020b)

Additionally, differences between ranks of coal influence mercury capture capabilities by air pollutant control devices (APCDs) because higher rank coals contain more chlorine, some forms of which react with mercury in flue gas when it passes through APCDs (Kolker et al., 2006). Chlorine and other halogen species promote the oxidization of mercury in homogenous and heterogeneous reactions under catalysis. When the content of chlorine and other halogen species in flue gas is high, mercury is more efficiently captured onto dust and in other ways by APCDs (Galbreath et al., 2000; Gale et al., 2008; Kolker et al., 2006). Numerous experiments have indicated that mercury removal rates increase when the concentration of HCl is increased (Cao et al., 2005; Gale et al., 2008; Sliger et al., 2000). Chlorine also promotes mercury oxidization when the temperature of flue gas is increased. In the experiments conducted by Sliger et al. (2000), the concentration of Hg(0) was less than 50 $\mu g/m^3$ when the test gas temperature was over 400 °C. When the test gas temperature was continuously increased to 900 °C, the concentration of Hg was less than 10 $\mu g/m^3$. Gao et al. (2013) and Masoomi et al. (2020) also reported similar results. When the temperature of process gas or the concentration of HCl present in process gas was increased, the Hg(0) oxidation rate increased (Gao et al., 2013; Masoomi et al., 2020). When the concentration of HCl in the test gas was high, it required the lower temperature of process gas for Hg oxidation, and vice versa (Li et al., 2017; Sliger et al., 2000).

The homogenous pathway of Hg(0) oxidation involves atomic $Cl^{\bullet}$, and the concentration of $Cl^{\bullet}$ depends on gas-phase reactions involving O_2, water vapor, hydrocarbons, chlorine compounds, and sulfur compounds (Abad-Valle et al., 2011). The relevant transformation process of chlorine is described by Equations (1) to (4) (Cao et al., 2005).

$$Cl^{\bullet} + H^{\bullet} \rightarrow HCl \quad (1)$$

$$2Cl^{\bullet} \rightarrow Cl_2 \quad (2)$$

$$4Cl^{\bullet} + 2H_2O \rightarrow 4HCl + O_2 \quad (3)$$

$$4HCl + O_2 \rightarrow 2Cl_2 + 2H_2O \quad (4)$$

Mercury released from solids into process gases reacts with chlorine species in Equations (5) to (8) (Cao et al., 2005).

$$Hg + Cl^{\bullet} \rightarrow HgCl \quad (5)$$

$$HgCl + Cl_2 \rightarrow HgCl_2 + Cl^{\bullet} \quad (6)$$

$$Hg + Cl_2 \rightarrow HgCl_2 \quad (7)$$

$$2Hg + 4HCl + O_2 \rightarrow 2HgCl_2 + 2H_2O \quad (8)$$

Different tapes of fly ash are produced in the combustion of mineral-organic wastes, lignite, anthracite, and subbituminous or bituminous coals. Predominant amounts of fly ash come from coal-fired power plants (CFPPs) and incineration plants. Ashes from process gas mainly contain SiO_2+Al_2O_3+Fe_2O_3+CaO (50–70%) (ASTM, 2010). Fe_2O_3 is a good catalyst for the heterogeneous transformation of mercury. When flue gas contains HCl, oxidation of mercury occurs at the surface of fly ash. The heterogeneous pathway of Hg(0) oxidation involves activation (chlorination) of unoccupied Hg(p) sites on Fe_2O_3. The relevant transformation

process of chlorine on the surface of fly ash was described by the chain of Equations (9) to (16), where $Cl^*_{(ad)}$ and $HgCl^*_{(ad)}$ represent unoccupied atoms or molecules adsorbed on the surface of the fly ash (Yang et al., 2016).

$$HCl \xrightarrow{Suface} Cl^*(ad) + H^{\bullet} \quad (9)$$

$$Cl^*_{(ad)} + Cl^{\bullet} \rightarrow Cl_2 \quad (10)$$

$$Cl^*_{(ad)} + Hg(0) \rightarrow HgCl^*_{(ads)} \quad (11)$$

$$Cl^*(ad) + Hg(0) \rightarrow HgCl^{\bullet} \quad (12)$$

$$Cl^*(ad) + HgCl^{\bullet} \rightarrow HgCl_2 \quad (13)$$

$$HgCl^*_{(ads)} + HCl \rightarrow HgCl_2 + H^{\bullet} \quad (14)$$

$$Cl^*(ad) + HgCl_2 \rightarrow HgCl^*_{(ads)} + Cl_2 \quad (15)$$

$$Cl^*(ad) + H_2O \rightarrow HCl + OH^{\bullet} \quad (16)$$

There are three main types of APCDs: those utilizing NO_x selective catalytic reduction or selective non-catalytic reduction (SCR, SNCR), (wet) flue gas desulfurization ((W)FGD), and particle controlling devices (PCDs), including electrostatic precipitators (ESP) of different kinds and fabric filters (FF). Removal of mercuric pollutants from flue gases is a side benefit of APCDs. The APCDs capturing mercury pollutants from flue gases in CFPPs are presented in Fig 2. Under heterogeneous or homogeneous reactions, the SCR device with its effective catalytic bed oxidizes Hg(0) with O_2, sulfur compounds and halogen species, etc. The remaining Hg(0) and oxidized mercury are emitted from the SCR device to the preheater. The remaining Hg(0) is continuously oxidized under the homogenous reaction in the preheater. The oxidized mercury, halogenated mercury, particulate matter bonded mercury, and partially Hg(0), are captured in the high voltage electrical field, inside ESP devices. The uncaptured mercury pollutants go into the WFGD system, where the soluble mercury pollutants are usually stopped by the system, and the non-soluble mercury pollutants mostly further escape. The uncaptured mercury is then released into the atmosphere. Many researchers have studied and investigated the removal of mercury from flue gas by APCDs through laboratory-scale experiments and full-scale plants, and found that each form of APCD, including SCR, ESP, FF, FGD, and wet electrostatic precipitators (WESP), had a positive effect on mercury capture from flue gas (Masoomi et al., 2020; Pavlish et al., 2003; Wang et al., 2009) Fig. 2. Total mercury removal from flue gas by ESP + FGD ranges from 27.48% to 81.36% (Gołaś and Strugała, 2013), by SCR + ESP + WFGD ranges from 63.54% to 74.11% (Su et al., 2017), and by SCR + ESP + WFGD + WESP ranges from 56.59% to 89.07% (Zhao et al., 2019a).

SCR devices oxidize the acidic and harmful NO_x gases to form neutral nitrogen gas. Ammonia gas (NH_3) or urea (CH_4N_2O) are common reactants used to reduce NO_x in flue gases of different kinds. The main deNO_x reaction in SCR devices is described by Equations (17) and (18).

$$4NO + 4NH_3 + O_2 \rightarrow 4N_2 + 6H_2O \quad (17)$$

$$6NO_2 + 8NH_3 \rightarrow 7N_2 + 12H_2O \quad (18)$$

The catalysts applied in SCR devices can be divided into two classes. The first class contains catalysts based on noble metals such as Pd, Au, Pt and Ag. Investigations of the potential oxidation of mercury in SCR devices revealed that Pd oxidized more than 95% of elemental Hg at an initial stage. The results also indicated that Pd could be readily regenerated, to improve oxidation activity, by heating it to approximately 315 °C for several hours (Hrdlicka et al., 2008; Presto et al., 2008). The second class contains catalysts that are based on transition metal oxides, such as tungsten oxide (WO_3) or vanadium pentoxide (V_2O_5) supported on titanium dioxide (TiO_2). The operational temperature of SCR devices when these metal catalysts are applied was around 280–400 °C. Under working conditions appropriate for SCR, V_2O_5 and TiO_2 promote Hg(0) oxidation reactions in presence of HCl, SO_2, and fly ash. Oxidized Hg^{2+} easily forms particulate bonded mercury and/or vaporous forms such as $HgCl_2$, HgO, $Hg(NO_3)_2$, $HgSO_4$ (Dranga et al., 2012; Gao et al., 2013). In the redox reactions of mercury and chlo-

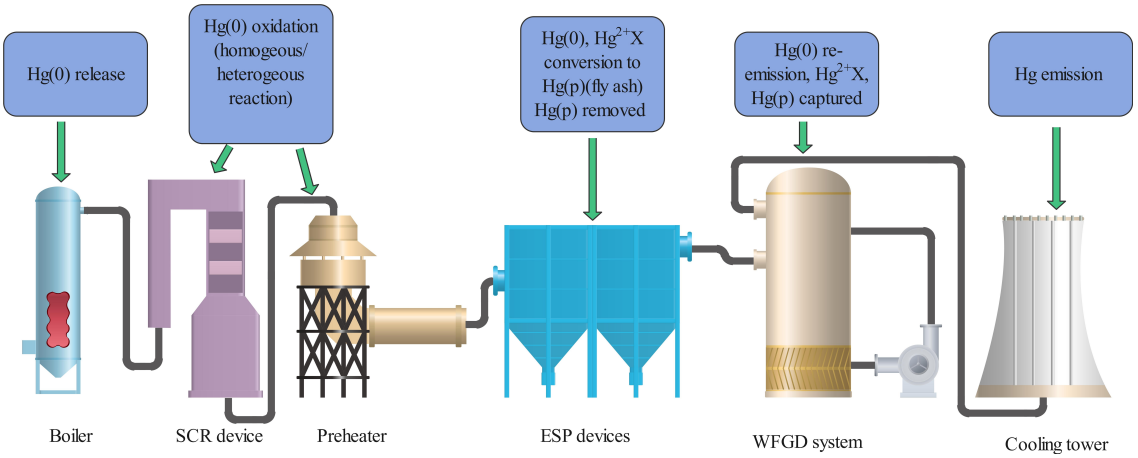

Figure 2. Transformation of mercury in flue gas through APCDs in CFPPs (Zhao et al., 2019a).

rine atoms, NO_x and NH_3 occur simultaneously on the active sites of the SCR catalyst (Zhang et al., 2016). Laudal et al. (2002) reported that SCR promoted Hg^{2+} from 6% to 26% in normal operation from both the inlet and outlet sides. Two more examples from the CFPPs in China were reported. The Hg(0) concentration in flue gas, before the inlet of the SCR, was 1.55 μg/m^3 and 5.73 μg/m^3, respectively. It diminished respectively to 1.02 μg/m^3 and 0.75 μ g/m^3, after the outlet of the SCR (Wang et al., 2010a; Liu et al., 2019). Also the data in Table 4 indicate that the concentration of Hg(0) decreases with SCR system. The rate of Hg(0) oxidation with the SCR system was 9.8 and 55.3% when low-chlorine coal and high-chlorine coal were burned, respectively (Li and Wang, 2021). In the SCR process, mercury undergoes oxidation through the Deacon reaction, the Eley–Rideal mechanism and the Langmuir–Hinshelwood mechanism, described in Sections 3.1 to 3.3.

The WFGD systems are used to capture SO_2 and SO_3 from flue gas, as well as water-soluble particles, by using the limestone-gypsum method. The data in Table 4 indicate that the rate of Hg^{2+} removal by the WFGD system is in the range of 48–98%. However, other researchers reported that Hg^{2+} removal by the WFGD system was in the range of 88.2–92.18% (Zhang et al., 2017b). Due to the high water-solubility of Hg^{2+}, the WFGD system has a high mercury co-capture ability. Particulate-bonded mercury and oxidized mercury are washed out and removed by limestone slurry and gypsum. Chen et al. (2014) demonstrated that the dissolved Hg^{2+} in limestone slurry continues to react with dissolved SO_2 to form $HgSO_3$, preventing the re-emission of the dissolved Hg^{2+}. The Hg(0) re-emission occurs during the Hg^{2+} removal process in WFGD devices. There are two reasons for this (Zhang et al., 2017b). Hg^{2+} and Hg(0) in flue gas generate Hg_2^{2+} on the surface of the limestone slurry layer. Then, Hg_2^{2+} reacts with OH^- in the limestone slurry to generate Hg(0) and HgO. SO_2 in flue gas can reduce HgO to form Hg(0). The relevant transformation process of Hg(0) and HgO can be described by Equations (19) to (21) (Zhao et al., 2017).

$$Hg^{2+}(aq) + Hg^0 \longleftrightarrow Hg_2^{2+}(aq) \quad (19)$$

$$Hg_2^{2+}(aq) + 2OH^- \longleftrightarrow H_2O + HgO + Hg^0(g) \quad (20)$$

$$HgO + SO_2(g) \longleftrightarrow Hg^0(g) + SO_3(g) \quad (21)$$

Table 4. Concentration of mercury species in flue gas from 6 different power plants.

Power plants	Hg species	Sampling location				Hg removal rate	Sources
		SCR inlet (μg/m^3)	ESP inlet (μg/m^3)	WFGD inlet (μg/m^3)	Stack (μg/m^3)		
P#1	Hg^T	24.49	19.22	0.77	0.60	94.4%	Liu et al. (2019)
	Hg(0)	5.73	0.75	0.33	0.49		
	Hg^{2+}	4.65	1.76	0.45	0.10		
	Hg_p	14.11	14.43	0.001	0.005		
P#2	Hg^T	1.92	1.89	1.44	1.22	36.5%	Wang et al. (2010a)
	Hg(0)	1.55	1.02	1.00	1.08		
	Hg^{2+}	0.15	0.40	0.44	0.13		
	Hg_p	0.22	0.47	0.00	0.00		
P#3	Hg^T		28.3	5.5	3.9	86.7%	Li and Wang (2021)
	Hg(0)		3.1	2.9	2.6		
	Hg^{2+}		2.9	2.5	1.3		
	Hg_p		22.3	0.1	0.01		
P#4	Hg^T	2.984	2.852	1.090	0.240	92%	Chou et al. (2021)
	Hg(0)	0.811	0.601	0.647	0.221		
	Hg^{2+}	0.07	0.192	0.397	0.008		
	Hg_p	2.102	2.058	0.047	0.016		
P#5	Hg^T		30.7	20.0	19.5	53.5%	Pilar et al. (2021)
	Hg(0)		12.5	15.8	15.3		
	Hg^{2+}		13.0	3.9	4.0		
	Hg_p		5.3	0.3	0.3		
P#6	Hg^T		16.2		0.24	98.53%	Li et al. (2019)
	Hg(0)		0.19		0.12		
	Hg^{2+}		0.62		0.12		
	Hg_p		15.3		0.00		

Hg^{2+} dissolved in a scrubber solution can react with sulfite or sulfate (resulting from SO_2 dissolving in a scrubber solution) to form $HgSO_3$ or $HgSO_4$. A portion of $HgSO_3$ or $HgSO_4$ may further participate in some reactions to release Hg(0). The relevant transformation process of Hg(0) release can be described by Equations (22) and (23) (Zhao et al., 2019a).

$$Hg^{2+}(aq) + SO_3^{2-}(aq) \rightarrow HgSO_3(aq) \rightarrow Hg^0(g) \quad (22)$$

$$Hg^{2+}(aq) + SO_4^{2-}(aq) \rightarrow HgSO_4(aq) \rightarrow Hg^0(g) \quad (23)$$

Moreover, Hg(0) re-emission is affected by operating temperature, pH, O_2 concentration in flue gas, and sulfite concentration, among other factors. It has been found that high availability of excess oxygen in flue gas in contact with desulfurization solution decreases the rate of reduction of Hg^{2+} to Hg(0), while decreasing the slurry pH or increasing the operating temperature enhances Hg(0) re-emission significantly. The relevant transformation process of Hg^{2+} and the relationship of Hg(0) with pH can be described by Equations (24) to (27) (Chang et al., 2017; Omine et al., 2012; Wu et al., 2010).

$$Hg^{2+}(aq) + SO_3^{2-}(aq) \rightarrow HgSO_3(aq) \quad (24)$$

$$Hg^{2+}(aq) + HSO_3^{-}(aq) + H^{+} \rightarrow HgSO_3(aq) + 2H^{+}(aq) \quad (25)$$

$$HgSO_3(aq) + H_2O(l) \rightarrow Hg^0(g) + SO_4^{2-} + 2H^{+}(aq) \quad (26)$$

$$HgSO_3(aq) + SO_3^{2-}(aq) \rightarrow Hg(SO_3)_2^{2-}(aq) \quad (27)$$

If a catalytic oxidizer or SCR devices is used upstream before the WFGD system, the WFGD techniques are much more effective in mercury removal. Finally, a part of the mercury load is captured by the limestone slurry and gypsum, as most of Hg(0) passes through the desulfurization system.

The ESP system is one of the particulate matter control devices used in CFPPs. It consists of a row of thin vertical wires and a stack of large, vertically-oriented flat metal plates. A negative charge of several thousand volts is applied between the wires and the plates. If the applied voltage is high enough, a corona discharge will ionize the air around the electrodes and then ionize the particles in the airflow, when the exhaust gas passes through the multiple plates of the ESP system. Most of solids are then attracted by the electrical plates, and finally collected. Oxidized mercury and particulate-bonded mercury can both be attracted by the high-voltage electrical charge. When flue gas passes through the electrical fields, the high-voltage electrical charge produces free radicals such as $O^{\bullet}$, $OH^{\bullet}$, O_3, $Cl^{\bullet}$, and Cl_2 from flue gas components. The relevant transformation process by which the ESP system produces free oxygen radicals can be described by Equations (28) to (32) (Chen et al., 2006; Niu et al., 2015).

$$e^{-} + O_2(g) \rightarrow O^{\bullet} + O^{\bullet} \quad (28)$$

$$O^{\bullet} + O_2 \rightarrow O_3 \quad (29)$$

$$H_2O + O^{\bullet} \rightarrow 2OH^{\bullet} \quad (30)$$

$$H_2O + O_3 \rightarrow H_2O_2 + O_2 \quad (31)$$

$$OH^{\bullet} + O_3 \rightarrow HO_2^{\bullet} + O_2 \quad (32)$$

Many researchers have studied the oxidization of mercury using ESP systems in the laboratory and in the field. When discharge voltages were increased from 5 kV to 7.5 kV with concentrations of O_2 and Hg(0) at 1% (v/v) and 50 μm^3, Hg(0) oxidation efficiency substantively increased to 74% (Niu et al., 2015). In the ESP system, mercury oxidation is dependent on the free radical content in flue gas. When O_2 concentration was increased from 1 to 7%, while the O_3 concentration was also increased from 0.158 to 1.169 g/m^3, the mercury oxidation rate increased from 78 to 86% (Niu et al., 2015). HCl plays an important role in oxidation of Hg(0). In process gas containing 30 ppm of HCl and 5% of O_2, the concentration of Hg(0) was decreased from 28.2 to 14.7 $\mu g/m^3$ within 30 min, and when the concentration of HCl in the process gas was increased from 30 to 60 ppm, the concentration of Hg decreased from 14.7 to 1.6 $\mu g/m^3$ within 15 min (Wang et al., 2010b). The relevant transformation process of mercury oxidation by free radicals can be described by Equations (33) to (40) (Chen et al., 2006; Niu et al., 2015; Wang et al., 2010b).

$$Hg(0) + O^{\bullet} \rightarrow Hg(0) \quad (33)$$

$$Hg(0) + O_3 \rightarrow Hg(0) + O_2 \quad (34)$$

$$e^{-} + HCl(g) \rightarrow H^{\bullet} + Cl^{\bullet} \quad (35)$$

$$Cl^{\bullet} + Cl^{\bullet} \rightarrow Cl_2(g) \quad (36)$$

$$Hg(0) + Cl^{\bullet} + M \rightarrow HgCl + M \quad (37)$$

$$HgCl + Cl^{\bullet} \rightarrow HgCl_2 \quad (38)$$

$$Hg(0) + Cl_2 + M \rightarrow HgCl_2 + M \quad (39)$$

$$Hg(0) + 2OH^{\bullet} \rightarrow Hg(OH)_2 \quad (40)$$

Sorbent injection, including activated carbons, is one of the solutions applied to improve the capture of pollutants from exhaust gas before ESP. The sorbent is injected into the exhaust gas upstream the ESP system, adsorbing the vaporous or gaseous pollutants onto its surface. When the exhaust gas passes through the ESP system, the injected sorbent with its adsorbed pollutants is collected on electrical plates. Wu et al. (2008) and Zhou et al. (2015a) increased mercury capture by establishing a laboratory-scale multiphase flow reactor with injected raw activated carbon, bromine modified activated carbon and other kinds of adsorbents. When the adsorbent was injected into their system, the concentration of oxidized mercury and elemental mercury in the simulated gas decreased from 5000 to 0 ng/m^3 (Wu et al., 2008). When

the injection process was stopped, the concentration of oxidized mercury and elemental mercury in the simulated gas increased again. In the other experiment, when flue gas contained over 5% of unburnt carbon (UBC) or activated carbons, around 80 to 90% of mercury was captured from exhaust gas (Gibb et al., 2000). Lee et al. (2006) also presented data on Hg(0) oxidation efficiency in laboratory-simulated gas conditions. The Hg(0) conversion rate in simulated gas containing 20 ppm HCl was 55% without fly ash injection, and the Hg(0) conversion rate when fly ash was injected into the simulated gas was 44%. Gale et al. (2008) reported that UBC increased from 0.71–0.73% to 1.45%, while the process gas contained 13.0 ppm of HCl. At the same time, Hg(0) removal efficiency increased from 33.6% to 57.5%.

However, the carbon injection technique has some drawbacks, such as the risk of polymerization of unsaturated hydrocarbons occurring in flue gas and its effect on the reuse of fly ash (Wdowin et al., 2020). UBC content in fly ash should not exceed 5%, if successfully used to construction materials, especially insulating concretes (Macherzynski, 2018). Therefore, zeolites and impregnated zeolites are considered to be the optimal option. The synthetic zeolites (Wdowin et al., 2015) and specific manganese oxide sorbents (Wiatros-Motyka et al., 2013) showed remarkable results of mercury removal in laboratory conditions. Both materials do not have the drawbacks of most activated carbons.

Although combinations of SCR, ESP, and WFGD devices can remove mercury pollutants to a large degree, their mercury capture efficiency is usually lower than that of specific mercury removal methods in CFPPs. SCR, WFGD, and ESP devices sometimes release, vaporize or reactivate mercury back to flue gas. In the SCR process, the by-reaction process takes place, where NH_3 inhibits the conversion of Hg(0), occupying the active sites instead of Hg(0). Hg^{2+} reacts with NH_3 to reform Hg(0) and HCl, N_2 downstream. The relevant transformation process of Hg^{2+} reduction back to Hg(0) by NH_3, can be described by Equation (41) (Stolle et al., 2014; Zhou et al., 2015b).

$$4HgCl_2 + 4NH_3 + O_2 \longrightarrow 4Hg(0) + 8HCl + 2N_2 + 2H_2O \quad (41)$$

Some WFGD systems may release mercury during processing, and Hg^{2+} dissolved in a scrubber solution can react with sulfite and sulfate to form $HgSO_3$ and $HgSO_4$. A portion of $HgSO_3$ and $HgSO_4$ may further participate in some reactions to release Hg(0); the relevant transformation processes are described by reactions (19) to (23) (Chen et al., 2014; Wu et al., 2010). Injected activated carbon (ACI) or UBC which reach fly ash may also release mercury after collection by ESP systems at high temperatures (Luo et al., 2006). Hence, full removal of elemental mercury from industrial flue gas often requires additional procedures or devices.

2.2. Mercury removal in metal production industries

Fossil fuels are used as the primary energy source for industrial production, and APCDs are implemented to reduce pollutant emissions from industry. Unlike power plants, nonferrous metal (Zn, Pb and Cu) factories utilize other devices to reduce NO_x in process gases, such as low NO_x burners (LNB). The APCD process as a whole in these plants consists of LNB and ESP + FGD or FF + FGD. LNB systems are designed to control air and fuel mixing at each burner, which creates larger and more branching flames. Typically, fly ash contains between 2% and 12% of UBC. After LNB technology was invented and installed in boilers, the amount of UBC in fly ash increased, even to 20% (Ahmaruzzaman, 2010). UBC adsorbs Hg(0) from flue gas to its surface, catalyzing mercury oxidation in the presence of HCl and other acidic gases (Hower et al., 2010). However, because these APCD processes lack catalysts, the rate of Hg oxidation and the rate of Hg(0) removal are both lower than in other APCD processes, for example SCR. Zhang et al. (2015) investigated the mercury emissions from the nonferrous metal (Zn, Pb and Cu) smelting plants. The total mercury emissions from this sector were 116.6, 21.2 and 8.6 tonnes, respectively. But the Hg(0) emissions from this sector were 52.9, 14.7 and 5.1 tonnes, respectively (Zhang et al., 2015).

Fukuda et al. (2011) investigated mercury emissions from ferrous production processes and found that 73% of the mercury input was emitted into the environment when ESP was used. Mercury emissions were reduced to 56% with the addition of a desulfurization process and to 34% with an active carbon process (Fukuda et al., 2011). The authors also compared the mercury removal rates of ferrous factories with those of municipal waste treatment plants and found that they were similar: 27% or 35% using ESP with or without the injection of alkaline reagent, respectively, and more than 90% with an active carbon process. This paper also notes that the average mercury removal rates were 80.6–86% in ferrous metal production in Japan (Fukuda et al., 2011).

Wang et al. (2016) investigated a typical iron plant and a typical steel plant in China and found that their Hg(0) emissions were 26.7% and 40.8%, respectively. They found that the sintering machine and coal gas burning produced the largest amount of mercury emissions, these accounted for 46–50% and 17–49% of total mercury emissions, respectively. ESP and desulfurization unit removed 24–85% of mercury emissions in the iron production process and 68–82% in the steel production process (Wang et al., 2016). More dedicated APCDs were applied in flue gas controlling processes, more mercury was captured. For instance, one sinter plant in Austria applied the FF and the WFGD and the polychlorinated dibenzo-p-dioxins and furans (PCDD/F). The mercury capture rate was 80–95% (Remus et al., 2013).

2.3. Mercury removal in cement plants

Cement production is an anthropogenic source of mercury emission to the environment. During cement production using the kiln system, mercury compounds are vaporized from fuels and raw materials because of the very high temperatures inside the kiln. The raw materials and fuels are milled separately and then mixed before being put into the kiln. The preheater and precalciner generate the flue gas. The mercury present in the raw materials and fuels is released as flue gas. Some of the mercury is adsorbed from the flue gas with a fabric filter before the particulate matter (PM) recycling system, and this part of mercury as a dust circulates back to the kiln system. The remaining mercury in the flue gas is collected by a particulate matter collector before it enters the stack. The gas phase of mercury in flue gas is adsorbed by the dust in the PM recycling system. And the collected dust is returned to the kiln system by the PM recycling system. Only some gas phase of mercury escapes from the PM recycling system and enters into the stack (Fig. 3, Kern et al., 2015).

Yue et al. (2013) studied four cement plants in China and found that the only pollutant control devices used in them were particulate control devices (PCDs) in the kiln system. The PCDs in downstream exhibited low mercury removal efficiency: mercury concentration was 2.5 to 5.4 times higher downstream of the kiln systems than it was upstream of the kiln systems (Yue et al., 2013). On the other hand, these cement plants did have PM recycling systems. The dust including PM-bonded mercury was returned to the kiln systems. The efficient removal of mercury by ESP or FF thus caused high mercury enrichment during the cement production process, which resulted in high mercury emissions (Wang et al., 2014). Wang et al. (2014) studied other three cement plants in China and found that the rates of mercury removal from flue gas in a raw mill + FF and a coal mill + FF were 87% and 94%, respectively, and that over 70% of the mercury in the flue gas was collected together with PM by the FF. Nevertheless, the mercury output/input ratios in these cement plants were 120%, 127% and 101%: the mercury that was removed was returned to the kiln by the PM recycling systems. As a result, over 90% of the mercury in the process was being released to the atmosphere (Wang et al., 2014). Chou et al. (2018) also had a similar conclusion with Wang et al. (2014). They reported that 97.5% and 86.5% of mercury input at raw mill ESP was Hg_p in the investigated plant 1 and plant 2, respectively. The inputs of Hg_p at raw mill stack was 1.4% and 1.1% in plant 1 and plant 2, respectively. The captured Hg_p backed to the raw mill silo system and it enriched a high mercury concentration in cement production process (Chou et al., 2018). This phenomena was also proofed by Li et al. (2022b), they found that the volatile metal, like Hg, had a significant high enrichment factor and it resulted in Hg being accumulated in production process (Li et al., 2022b).

2.4. Mercury removal in waste incinerators

Municipal solid waste (MSW) is an anthropogenic source of mercury emissions. Although mercury emissions from MSW incineration plants (MSWIPs) are much lower than mercury emissions from ASGM and fossil fuel combustion in power plants and cement plants (Table 1), total mercury emissions from MSW incinerators are significant and cannot be ignored. In the USA, 11.39–22.05% of total mercury emissions from MSWIPs were in the form of elemental mercury. The APCDs in these MSWIPs were spray absorber + big filter and spray dry absorber + big filter + SCR (Park et al., 2008). The total

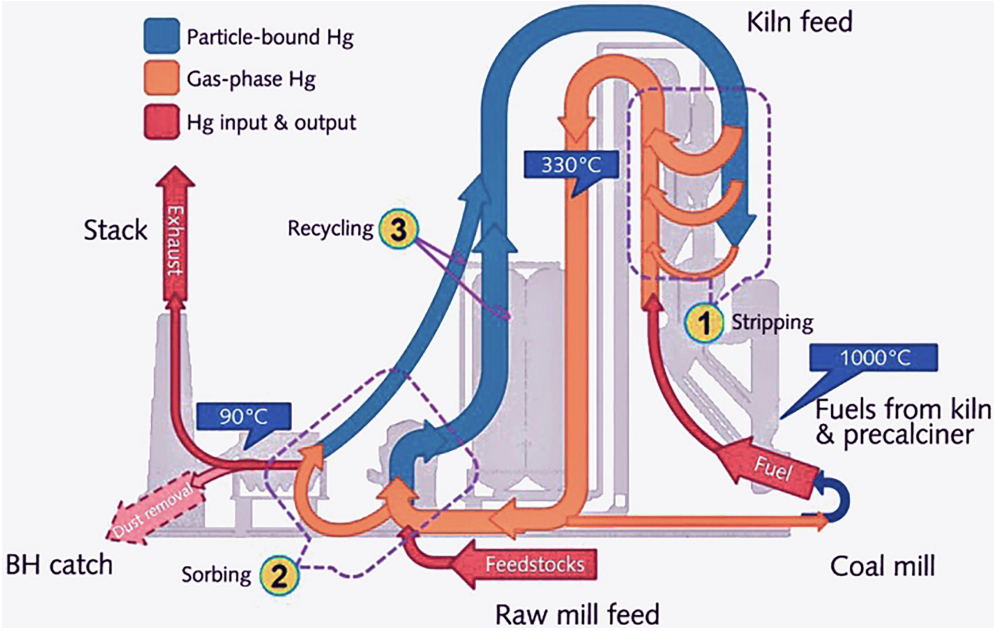

Figure 3. Mercury cycle in a cement plant (Kern et al., 2015).

mercury emissions from MSWIPs were 10.4 tonnes in 2003 in China, and 96% of total mercury emissions in the form of elemental mercury (Zhang et al., 2015). The main form of mercury flux in raw flue gases, in both investigated MSWIPs, is particulate-bonded mercury (Zhang et al., 2016). This form of mercury is easily removed with APCDs. Although total mercury emissions from MSWIPs were reduced by over 80% in China between 2003 and 2010, the main form of these emissions remains elemental mercury (Zhang et al., 2015).

The methodology of mercury removal is similar, both in MSWIPs and CFPPs. Typically, APCD employed in a MSWIP is a part of a combined pollution control strategy. Dry or semi-dry FGD is applied to remove SO_2 and HCl+HF. ESP and FF dust collectors are used, sometimes in combination with wet scrubbers (WS) and other technologies (Park et al., 2008; Zhang et al., 2015). SCR and ACI systems are implemented to remove NO_x, heavy metals and persistent organic pollutants (POPs). A single APCD was applied to remove mercury from process gas in the MSWIP. The mercury removal efficiency with ESP, FF, WS was 20.4%, 53.0% and 77.8%, respectively (Hu et al., 2018). The combined different types of APCD in the same plant showed higher mercury capture rates. The mercury removal efficiencies determined with fixed bed adsorber (FBA) + WS, ESP + FBA, ESP + FF + WS + dry sorbent injection (DSI) were 96.2%, 95.6% and 94.9%, respectively (Hu et al., 2018). The strategy resulting in mercury removal rates in the range of 33.6–95.2% was also reported by Li et al. (2018). Differences in mercury removal efficiencies can potentially be attributed to the operation of APCDs and to levels of mercury content in waste (Li et al., 2018). Takahashi et al. (2012) reported that waste plastic incinerators, sewage treatment sludge (STS) incinerators and combined STS and waste plastic incinerators, equipped with FF, had mercury removal efficiency rates of 34%, 92% and 84%, respectively. Industrial waste incinerators equipped with WS + WESP had a mercury removal efficiency rate of 92.7% (Takahashi et al., 2012). This result is close to the data published by Park et al. (2008). Industrial waste incinerators equipped with dry or semi-dry scrubbers (DS or SDS) + FF exhibited mercury removal rates in the range of 96.3– 98.7% (Park et al., 2008).

3. MECHANISMS FOR MERCURY CAPTURE FROM PROCESS GASES

The surface reactions of adsorbents defined by Langumuir take place in three distinct ways, each of which may exhibit unique forms of activity due to the large number of active sites: (1) catalyst surface is involved in the chain of reactions and interactions between molecules or atoms coming from a gas phase, which adsorbed at neighboring areas create new bonds, and finally desorb, (2) reactions can occur between the adsorption layer and the atoms of the solid or (3) reactions can occur as a direct result of gas molecules colliding with adsorbed molecules or atoms on the sorbent or catalyst surface. Langmuir defined the surface coverage with the gas molecules with Equation (42):

$$\theta = KP/(1 + KP) \tag{42}$$

where P is the gas pressure and K is the equilibrium constant for adsorption-desorption (Prins, 2018).

As mentioned before, catalysts and adsorbents employed in industry are frequently involved in mercury oxidation and capture processes in process gas. Two types of sorption may take place when capturing contaminants: physisorption and chemisorption. In physisorption, sorbents such as activated carbon and zeolites adsorb pollutants from flue gas by means of the Van der Waals forces or their distinctive structure, allowing for the selection of contaminants based on their size. Because sorbents adsorb pollutants on their surface by means of week physical forces, they may be quickly rendered ineffective, when the temperature or pressure changes. Hence, at higher temperature of process gases, physisorption is of less importance. Chemisorption employs chemical bonds between the adsorbent surface and the contaminants. At the initial stage, pollution is adsorbed by sorbents, then it is followed by formation of chemical bonds with the sacrificial ions of the sorbent.

Hg(0) vapors released as a result of combustion can be converted to Hg^{2+} through homogeneous (gas–gas) or heterogeneous (gas–solid) processes. The interaction with gas-phase chlorine to create $HgCl_2$ is the principal homogeneous oxidation process. Although this reaction has a favorable thermodynamic profile, it has a kinetic limit. Heterogeneous oxidation reactions are thought to occur on the surface of fly ash and UBC (Srivastava et al., 2006). Thus, the heterogeneous Hg/Cl mechanism on UBC surface is postulated as reactions (9) to (15) stated in Section 2, which are typical chemical processes of the Deacon mechanism (Section 3.1).

The adsorption and oxidation of mercury on catalyst surface has been the subject of a number of studies. It is well established that Hg(0) can undergo heterogeneous or homogeneous reactions in SCR systems. The effect of SCR catalysts on Hg(0) oxidation has been extensively explored in order to gain a better understanding of the mechanisms driving Hg(0) oxidation. However, the precise mechanisms of mercury oxidation on SCR catalysts, as well as their influence on flue gas characteristics, are yet to be clarified (Cao et al., 2005; Du et al., 2014; Hisham and Benson, 1995; Yang et al., 2016; Zhang et al., 2020).

Several mechanisms have been proposed to explain heterogeneous Hg(0) oxidation, including the Deacon process, the Eley–Rideal mechanism, the Langmuir–Hinshelwood mechanism, and the Mars–Maessen mechanism (Fig. 4). In these chemisorption mechanisms, pollutant ions react with metals on the sorbent in two different ways. In the first way, pollutant ions are adsorbed onto sorbents, after which they continue to

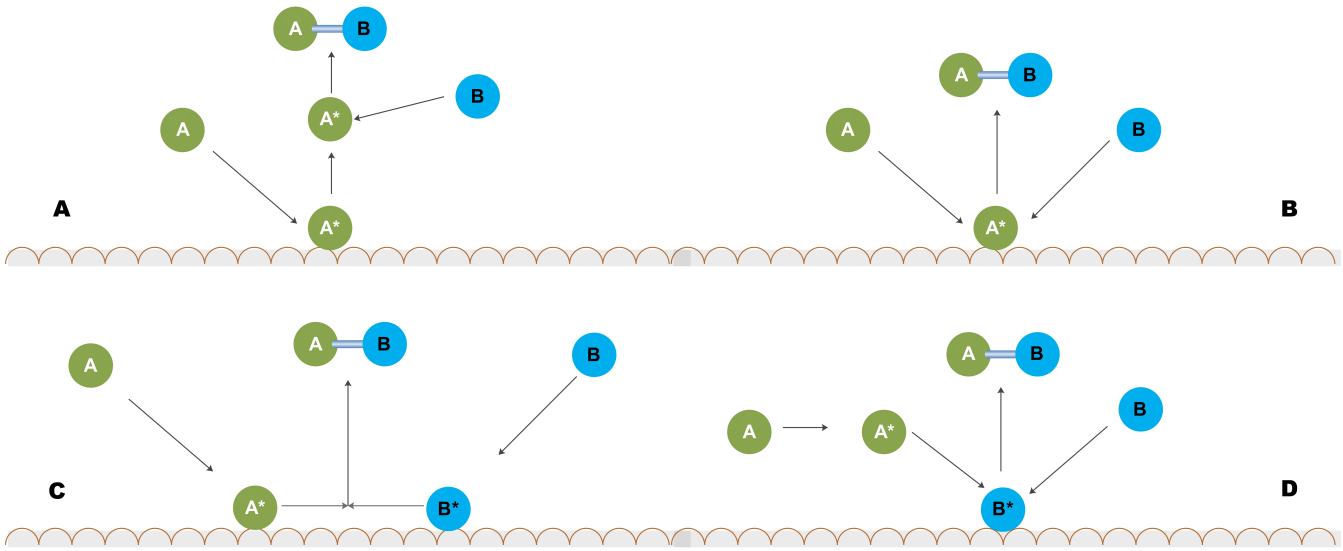

Figure 4. The mechanisms of atoms transformation, where A is Deacon mechanism, B is Eley–Rideal mechanism, C is Langmuir–Hinshelwood mechanism, and D is Mars–Maessen mechanism (Becker, 2018).

react with metals placed on the sorbent to establish a stable molecule, which can then be removed in a subsequent procedure. In the second way, pollutant ions react directly with a metal placed on the sorbent's surface, forming a chemical bond without the adsorption. The Mars–Maessen process and the Langmuir–Hinshelwood mechanism are examples of the first chemisorption mechanism, while the Eley–Rideal and Deacon mechanisms are examples of the second.

3.1. Deacon mechanism

The Deacon reaction processes are based on the oxidation of hydrochloride or chlorine gas on the surface of the sorbent– the overall Equation (8) – which occurs at a temperature of 400–450 °C, in the presence of a catalyst (Cao et al., 2005; Hisham and Benson, 1995). Catalysts such as copper, iron, and manganese salts are acceptable for use in the Deacon process (Du et al., 2014; Zhang et al., 2020). Cl_2 and HCl adsorb on the catalyst, oxidizing Hg(0) as it passes through the sorbent surface. With a proper catalyst, the Deacon process is capable of converting large quantities of HCl to Cl_2, and the Cl_2 produced is a critical factor in the oxidation of mercury in flue gas. The Deacon reaction fundamental thermochemistry over a wide range of groups and transition metal oxides was studied by Hisham and Benson (1995). The process is composed of two independent steps: (1) HCl adsorption by the metal oxide to form metal chloride (or oxychloride) with water and (2) chloride oxidation by O_2 to regenerate the metal oxide and free Cl_2 – Equations (43) and (44):

$$M_xO_{x/2}(s) + xHCl(g) \rightarrow xMCl(s) + \frac{x}{2}H_2O(g) \quad (43)$$

$$2MCl(s) + \frac{1}{2}O_2 \rightarrow M_2O(s) + Cl_2(g) \quad (44)$$

The oxidized mercury Hg^{2+} easily undergoes further reactions in the flue gas. The Deacon reaction can also be described by the following steps: hydrogen subtraction from HCl, atomic chlorine recombination, hydroxyl recombination, water desorption, and dissociative oxygen adsorption. Then the chloride radical reacts directly with the gas phase of Hg(0) (Fig. 4A) (Hisham and Benson, 1995). These processes are similar to the homogenous Deacon process described by Equations (1) to (4) (Cao et al., 2005) and to the Mars–Maessen mechanism (Zhao et al., 2015).

3.2. Eley–Rideal mechanism

In contrast to the Langmuir–Hinshelwood process (Section 3.3), in the Eley–Rideal mechanism only one kind of atom or molecule is adsorbed onto the surface of sorbent, for instance the Hg(0) atom or HCl gas. If Hg(0) atoms remain in the gas phase, they react with the hypothetical adsorbed reactant to produce molecules, which readily desorb (Fig. 4B). Senior and Linjewile (2003) hypothesized that mercury oxidation may take place when the process gas passes though the SCR catalyst, via an Eley-Rideal mechanism. This mechanism involves chlorine compounds as intermediates (Dranga et al., 2012; Presto et al., 2008; Zhang et al., 2016). For instance, HCl competes with NH_3 on the catalyst adsorption. Then, HCl is adsorbed onto the catalyst to generate active sites, it reacts with gaseous Hg(0). In some cases, adsorbed HCl or the $Cl^{\bullet}$ also react with the weakly bound Hg(0) (Dranga et al., 2012; Senior and Linjewile, 2003; Wu et al., 2019). These processes are described by Equations (45) and (46).

$$HCl(g) \longleftrightarrow HCl(ad) \quad (45)$$

$$HCl(ad) + Hg^0(g) \rightarrow HgCl_2(g) \quad (46)$$

Senior and Linjewile (2003) also proposed another type of Eley–Rideal process. Hg(0) competes with NH_3 on the catalyst's active sites, and then adsorbed Hg(0) interacts with gaseous HCl. But in some cases, V_2O_5-based SCR catalysts may oxidize the adsorbed Hg(0) to Hg^{2+}, leading to the dissociative adsorption of HCl on catalyst's active sites. The chemically adsorbed chlorine radical then interacts with gas-phase Hg(0) to produce an intermediate HgCl, which then reacts with chlorine species to produce $HgCl_2$ (Dranga et al., 2012).

3.3. Langmuir–Hinshelwood mechanism

The bimolecular reaction taking place on a surface can be described by the Langmuir–Hinshelwood mechanism, when mercury atoms require an adsorption site on the sorbent's surface. This process involves two stages: first, mercury in a gas is adsorbed on a sorbent surface, and subsequently mercury and other oxygen-containing molecules interact with the sorbent surface. At the same time, mercury interacts with oxygen atoms or other ions on the sorbent's surface, resulting in the formation of Hg^{2+}. The byproducts desorb from the solid surface once the reaction is finished (Fig. 4C) (Zhao et al., 2015). The reactions in the Langmuir–Hinshelwood mechanism for oxidation of Hg(0) over a copper-based catalyst are described by Equations (47) to (50) (Zhang et al., 2020).

$$Hg^0(g) \rightarrow Hg^0(ad) \quad (47)$$

$$HCl(g) \rightarrow Cl^-(ad) + H^+(ad) \quad (48)$$

$$Cl^-(ad) + Cu^{2+} \rightarrow Cl^*(ad) + Cu^+ \quad (49)$$

$$Hg^0 + 2Cl^*(ad) \rightarrow HgCl_2(g) \quad (50)$$

3.4. Mars–Maessen mechanism

The Mars–Maessen mechanism is a similar to the Langmuir–Hinshelwood mechanism. Hg(0) is initially adsorbed on the surface of a sorbent or catalyst, then the adsorbed Hg(0) is oxidized by surface oxygen to form HgO. For instance, Hg(0) bonds with lattice oxygen and/or chemisorbed oxygen on the V_2O_5 catalyst surface to form the weakly bonded species Hg–O–V–O_{x-1}, which is then converted to HgO. During the oxidation of Hg, the vanadium oxidation state is converted from V^5 to the V^{4+}, which consumes the catalyst's lattice oxygen (Zhang et al., 2014). Gas-phase O_2 can be used to replace the consumed lattice oxygen and/or surface oxygen (Ling et al., 2015). Adsorbed mercury oxide reacts with a lattice oxidant (either O or Cl) supplied from the gas phase in this process, creating a binary mercury oxide (HgM_xO_{y+1}) (Fig. 4D) (Granite et al., 2000). Equations (51) to (55) demonstrate the Mars–Maessen mechanism for the oxidation of adsorbed mercury with a lattice oxidant – metal oxide catalyst (Granite et al., 2000; Zhao et al., 2015).

$$Hg(g) \xrightarrow{Surface} Hg(ad) \quad (51)$$

$$Hg(ad) + M_xO_y \rightarrow HgO(ad) + M_xO_{y-1} \quad (52)$$

$$M_xO_{y-1} + \frac{1}{2}O_2(g) \rightarrow M_xO_y \quad (53)$$

$$HgO(ad) \rightarrow HgO(g) \quad (54)$$

$$HgO(ad) + M_xO_y \rightarrow HgM_xO_{y+1} \quad (55)$$

The Mars–Maessen method has been extensively utilized to demonstrate the oxidation of mercury on metal oxide catalysts (Dranga et al., 2012; Fan et al., 2012; Zhang et al., 2020). Ling et al. (2015) reported a series of mercury capture processes using copper-based sorbents that employ the Mars–Maessen mechanism. These are described by Equations (56) to (63) (Ling et al., 2015).

$$Cu^{2+} + O^{2-} + HCl \longleftrightarrow Cu^+ + Cl^- + OH^- \quad (56)$$

$$Cu^+ + O^{2-} + HCl \longleftrightarrow Cu^0 + Cl^- + OH^- \quad (57)$$

$$Cu^+ + O_2 \longleftrightarrow Cu^{2+} + O^{2-} \quad (58)$$

$$OH^- + OH^- \longleftrightarrow H_2O + O^{2-} \quad (59)$$

$$Hg^0 + Cl^- \longleftrightarrow HgCl^- \quad (60)$$

$$HgCl^- + Cl^- + e^- \longleftrightarrow HgCl_2 \quad (61)$$

$$HgCl_2(g) \longleftrightarrow HgCl_2(ad) \quad (62)$$

Total reaction:

$$Hg + 2HCl + \frac{1}{2}O_2 \longleftrightarrow HgCl_2 + H_2O \quad (63)$$

4. THE IMPACT OF SULFUR COMPOUNDS ON MERCURY CAPTURE IN PROCESS GASES

Sulfur compounds in process gases have different effects on Hg(0) capture. When Hg^{2+} is dissolved in limestone slurry, it reacts with dissolved gaseous SO_2 to form mercury sulfites ($HgSO_3$), which are not stable substances in WFGD systems. In most conditions, $HgSO_3$ decomposes to Hg(0) immediately. These reactions were described in Section 2, Equations (19) to (27) (Chen et al., 2014). Data from some CFPPs prove Hg(0) reemission in WFGD systems (Table 4). SO_2 often inhibits Hg(0) oxidation by competing with HCl or Cl_2, occupying the adsorption sites or active surface of catalysts or even reacts with the sorbents (metal oxides, such as CuO or Al_2O_3, turned out to be the excellent sorbents for SO_2 and Hg(0) capture (Li et al., 2015; He et al., 2020)). A high SO_2 concentration in the process gas inhibited Hg(0) removal efficiency because SO_2 reacted with surface oxygen of copper based sorbents to form the thermally stable copper sulfates (Y. Xie et al., 2015; He et al., 2020). The assumed

chemical reaction between SO_2 and sacrificial CuO is described by Equation (64)

$$CuO + SO_2 + \frac{1}{2}O_2 \rightarrow CuSO_4 \quad (64)$$

On the other hand, some researchers have found that SO_3 in the process gas had a positive influence on mercury capture. Zhou et al. (2015b) reported that adsorbed SO_3 on UBC surface reacted with water vapor to generate H_2SO_4. The adsorbed H_2SO_4 reacted with Hg^{2+} in process gas to form $HgSO_4$ (Zhou et al., 2015b). Zhou et al. (2019) noted that SO_3 also impacted magnetic biochar (MBC): the adsorption sites of MBC and the process of Hg(0) removal was significantly hindered by SO_3, and the efficiency of Hg(0) oxidation increased with an increase of SO_3 concentration. The inhibitory effect of SO_3 on Hg(0) adsorption is attributed to competitive adsorption between SO_3 and Hg(0) and the formation of metal sulfates on the surface of MBC (Zhou et al., 2019). The Hg(0) oxidation with SO_3 over the V_2O_5/TiO_2 catalyst (the typical catalyst applied in SCR system) was proven by Yang et al. (2021b). They found that direct and indirect oxidation processes of Hg(0) took place on the catalyst. In the direct process, SO_3 was transformed into SO_4 and then reacted with mercury to $HgSO_4$. In the indirect process, Hg(0) was transformed to HgO with oxygen, then it reacted with SO_3 to form $HgSO_4$.

Nowadays, the coal gasification is a more popular and acceptable technology by using fossil fuel than conventional CFPPs. It provides more clean and high efficiency energy compared with CFPPs (Sultanguzin et al., 2020). But the syngas contains a much higher amount of Hg(0) compared with the exhaust gas from the CFPPs. The mercury mainly remains in the form of Hg(0) vapors during the coal gasification process (Altaf et al., 2022; Wang et al., 2020b; Zheng et al., 2021). H_2S is another pollutant from coal-derived or biomass-derived syngas (Marcantonio et al., 2020; Puig-Arnavat et al., 2010; Rahim et al., 2023; Villarini et al., 2019). A methodology for simultaneous removal of Hg(0) and H_2S from such process gases is advantageous and required. The metal oxides or carbon based metal oxides are a good option. They promote the interaction between the H_2S and Hg(0) in the process gas to form the non-water-soluble HgS (Altaf et al., 2022; Wang et al., 2020b).

The oxidation of Hg(0) by H_2S gas on the metal oxide surfaces may occur via Langmuir–Hinshelwood or Eley–Rideal processes. In the Langmuir–Hinshelwood mechanism, the H_2S molecule adsorbs on the metal oxide sorbent surface. Then the lattice oxygen is activated. The lattice oxygen reacts with the H_2S to form the activated sulfide layer on the sorbent surface. Hg(0) adsorbed onto the sorbent reacts with the sulfides and forms mercury sulfides (Fig. 5a) (Wang et al., 2018; Xing et al., 2022). This mechanism is described by the following postulated Equations (65) to (68):

$$H_2S(g) \rightarrow H_2S_{(ads)} \quad (65)$$

$$H_2S(ads) + O_\alpha \rightarrow S^{\bullet}(ads) + H_2O \quad (66)$$

$$Hg(g) \rightarrow Hg(ads) \quad (67)$$

$$S^{\bullet}(ads) + Hg(ads) \rightarrow HgS(ads) \quad (68)$$

In accordance to the Eley–Rideal mechanism, the H_2S molecules are adsorbed on the metal oxide sorbent's surface. Then the lattice oxygen is generated from the sorbent's surface. The lattice oxygen reacts with the H_2S to form the activated sulfide load on the sorbent's surface. The activated sulfide react with Hg(0) from the process gas without the mercury adsorption process (Fig. 5b). The interaction between Hg(0) and H_2S occurs in a similar way to Hg(0) oxidation when HCl is present. In this case, the activated surface sulfur reacts with gas phase Hg(0) to create stable HgS. Consequently, there are some proposed Equations from (69) to (71) (An et al., 2023; Wu et al., 2021; Xing et al., 2022; Xue et al., 2015):

$$H_2S(g) \rightarrow H_2S(ads) \quad (69)$$

$$H_2S(ads) + O_\alpha \rightarrow S^{\bullet}(ads) + H_2O \quad (70)$$

$$S^{\bullet}(ads) + Hg(g) \rightarrow HgS(ads) \quad (71)$$

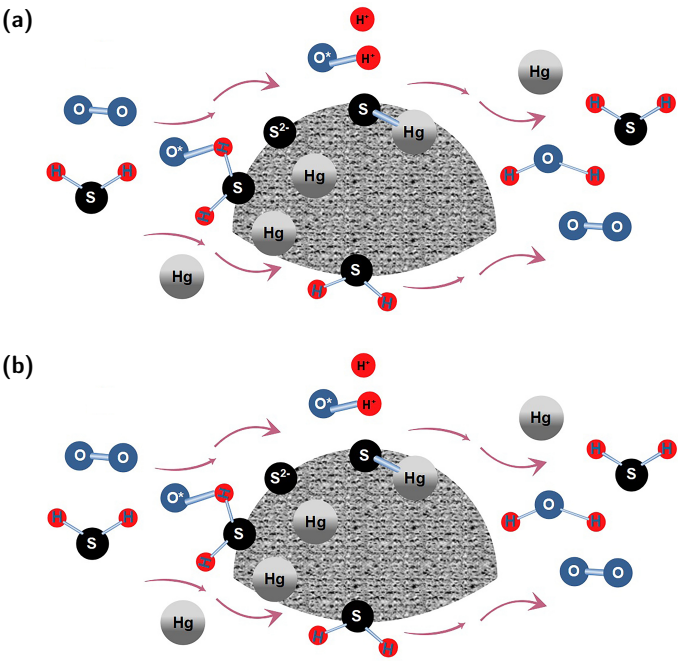

Figure 5. The processes of Hg(0) transformation by H_2S gas, where (a) is Langmuir–Hinshelwood mechanism, (b) is Eley–Rideal mechanism.

Wang et al. (2018) used the MnO_2 sorbent to investigate the influence of H_2S on Hg removal in simulated gas. They report that the H_2S promoted Hg(0) removal efficiency over

the MnO_2 sorbent. The effectiveness of Hg(0) capture was increased from 82.3% to 90.5%, when the temperature was increased from 80 °C to 160 °C, in the 400 ppm H_2S gas solution in N_2. The Hg(0) removal efficiency was decreased while the temperature of simulated gas was increased from 160 °C to 200 °C. This result was higher than the experiment conducted under the pure N_2 conditions (Wang et al., 2018). Wang et al. (2018) also indicated that the Hg(0) removal efficiency was increased from 85.9 to 96.9%, while the concentration of H_2S was increased from 200 to 800 ppm in the simulated gas. Wu et al. (2021) and Xing et al. (2022) also had similar reports. The Fe_2O_3 or Fe_2O_3/TiO_2 mixture sorbents showed a great Hg(0) capture rate in a temperature range of 100 to 150 °C when H_2S was present in the simulated gas (Wu et al., 2021; Xing et al., 2022). This temperature range was also an optimal range for H_2S removal using Fe_2O_3/AC sorbent. The Fe_2O_3/AC sorbent captured the H_2S from the simulated gas, H_2S performed as the active site on the sorbent. And then it reacted with Hg(0) from the simulated gas (Wang et al., 2022) But Xing et al. (2022) also noted that other gas components in the simulated gas, such as CO, H_2 and H_2O, inhibited the Hg(0) removal efficiency. Nevertheless, they showed over 80% of the Hg(0) capture rate (Xing et al., 2022).

Except for the gas phase sulfur compounds, having an effect on Hg(0) capture, sulfur solid compounds and sulfur derived modifications onto sorbents are good materials for Hg(0) removal from process gases. Metal sulfides, particularly CuS and FeS_2, are good options for Hg(0) capture in process gases. The acidic gas components, NO and SO_2, compete with Hg(0) to adsorb onto different active surfaces, but the metal sulfide sorbents' microstructure resists these gas components, and keep the Hg(0) removal efficiency in a range of 20–100% (Li et al., 2018; Liu et al., 2020; Xu et al., 2021). Liu et al. (2019) also noted that CuS can capture Hg(0) from process gas containing a high concentration of SO_2. They tested the Hg(0) adsorption capacity of CuS in 500 ppm, 1000 ppm and 2500 ppm SO_2 conditions. The Hg(0) adsorption capacity of CuS was 16.25 mg/g, 15.93 mg/g and 15.88 mg/g, respectively. The Hg(0) adsorption capacity of CuS in pure N_2 conditions was close to 17 mg/g (Liu et al., 2019). Our recent study had similar results with Liu et al. (2019). CuS showed over 97% of Hg(0) removal efficiency in the simulated gas without SO_2. There was no significant change of Hg(0) capture rate within one hour experiment when the simulated gas contained 1000 ppm of SO_2 (Deng and Macherzynski, 2022; Gorecki et al., 2022). Yang et al. (2021b) tested three kinds of metal sulfide sorbents, $CuFeS_2$, CuS, FeS_2 in different temperatures. These three sorbents showed remarkable results in a temperature range between 40 °C and 100 °C. 10 mg quantity of $CuFeS_2$ removed almost 100% of Hg(0) from the simulated gas containing 2000 ppm of SO_2 (Yang et al., 2021a). The mechanisms of Hg(0) removal with CuS followes the Mars–Maessen processes (postulated Equations (72) to (74)):

$$Hg(g) \rightarrow Hg(ads) \tag{72}$$

$$Hg(ads) + Cu^{2+} \rightarrow HgS + Cu \tag{73}$$

$$Hg(ads) + S_2^{2-} \rightarrow HgS + S^{2-} \tag{74}$$

The sulfate-reducing bacteria (SRB) were found in the WFGD systems (Brown et al., 2012; Martin et al., 2021). The SRB and the FGD sludge mixture fixes the heavy metal ions, such as As, Se, from the wastewater because it acts as an electron acceptor to generate H_2S (Liu et al., 2021; Okonji et al., 2021; Maiti et al., 2019), as well as fix the Hg^{2+} and prevent the Hg(0) reemission from sewer treatment systems (Yan et al., 2019). Some moderately thermophilic SRB had a good growth rate in the temperature range of 50 °C to 70 °C (Cha et al., 2013; Krukenberg et al., 2016). This temperature range was typically optimal for WFGD chemistry performance (Neveux et al., 2014; Yang et al., 2021c). Microbial activities might enhance SO_2 capture and gypsum formation (Tang et al., 2009; Zhang et al., 2017a). These observations might be the hint of the SRB biotechnique implementation in industries. The SRB activities that might influence Hg(0) capture and reemission were described in Equations (75) to (79) (Tang et al., 2009; Zhang et al., 2017a).

$$SO_2 + H_2O \rightarrow SO_3^{2-} + H^+ \tag{75}$$

$$SO_3^{2-} + O_2 \rightarrow SO_4^{2-} \tag{76}$$

$$SO_4^{2-} + 8e^- + 4H_2O \rightarrow S^{2-} + 8OH^- \tag{77}$$

$$Hg^{2+} + S^{2-} \rightarrow HgS \tag{78}$$

$$Hg(g) + S^{2-} \rightarrow HgS \tag{79}$$

The mechanisms of SRB involved enzymatic reduction and oxidation to remove the Hg(0) are described by Equations (80) to (86), APS: adenosine 5′-phosphosulfate;AMP: adenosine mono-phosphate (Xu and Chen, 2020).

$$2CH_3CHOHCOO^- + SO_4^{2-} + 4H_2O \rightarrow 2CH_3COO^- + 2HCO_3^- + HS^- + H^+ \tag{80}$$

$$2CH_3CH_2OH + SO_4^{2-} \rightarrow 2CH_3COO^- + HS^- + H^+ + 2H_2O \tag{81}$$

$$CH_3COO^- + SO_4^{2-} \rightarrow 2HCO_3^- + HS^- \tag{82}$$

$$AMP^{4-} + SO_4^{2-} + H^+ \rightarrow APS^{2-} + HP_2O_7^{3-} \tag{83}$$

$$APS^{2-} + 2e^{2-} + H^+ \rightarrow HSO_3^- + AMP^{2-} \tag{84}$$

$$HSO_3^- + 6e^{2-} + 6H^+ \rightarrow HS^- + H_2O \tag{85}$$

$$Hg^{2+} + H_2S \rightarrow HgS + 2H^+ \tag{86}$$

In laboratory studies, Huang et al. (2019) used membrane filters inoculated with the microbial culture containing enriched SRB, to design a bio-filter. The bio-filter worked in gas-liquid mode. It exhibited long-term Hg(0) bio-removal

efficiency in a range of 76.7–93.3% from the process gas. In addition, the bio-filter bioaccumulated 64.9% of Hg(0) loading, where 51.3% was HgS and 13.6% was in the humic/fulvic acid bound mercury form (Huang et al., 2019). The biotechnique application of SRB for Hg(0) removal in industrial settings still requires a lot of effort to understand. This is because the bioremediation of mercuric species includes enzymatic reduction and oxidation, and possible H_2S co-production. It was for instance responsible for the foaming in the WFGD system and the corrosion of steel structure (Brown et al., 2012). The SRB do not only transfer Hg(0) and Hg^{2+} into HgS, they also transfer mercury species to more toxic organic mercury, such as methylmercury (Hsu-Kim et al., 2013). And the SRB biomechanisms were unlike the four mechanism (Fig. 4), which are much better understood. It needs more studies to Figure out the SRB activities, and how this system prevents the Hg(0) emissions and if organic mercury is not produced in some implementation for industries.

5. SUMMARY AND CONCLUSIONS

This research reviewed the different mechanisms of elemental mercury oxidation and the principal mechanisms of mercury capture in process gases of different kinds. Anthropogenic processes are important sources of mercury emissions around the world. CFPPs are the primary source of mercury emissions into the atmosphere, along with cement plants and metallurgical plants, particularly in Poland, China, India, and the United States. In accordance with decarbonization and circular economy policies, many nations have imposed strict limitations on mercury emissions from energy generation and industrial production. However, fossil fuels will be still used as the primary and/or rather major energy source in some developing countries, and in indispensable industries, in the near future. The Hg(0) removal from CFPPs was well studied recently, but the Hg(0) removal from coal-derived or biomass-derived syngas still needs more work. Especially, the use of metal oxide sorbents or other technologies to remove both H_2S and Hg(0) from the process gases. The use of SRB in the biotechnique for Hg(0) bio-removal could be a hint for the next generation techniques.

1. Mercury species (speciation) and its variations in each process gas are responsible for most chemical and sorption activities in combustion exhausts. Mercury has been demonstrated to be a highly active and mobile element in coals and other fuels. The majority of mercury in these fuels immediately volatilizes to the gas phase. Post-combustion, elemental mercury interacts with flue gas components, partially forming gaseous oxidized mercury and particulate-bound mercury compounds.
2. APCDs have co-beneficial effects on mercury reduction when removing other pollutants such as NO_x, PM, SO_2, and fine PM, capturing between 36.5% and 98.53% of total mercury. Mercury removal effectiveness was calculated on the basis of APCD operations and mercury content in wastes (Table 5) (Park et al., 2008; Zhang et al., 2015; Zhang et al., 2016).
3. Natural mercury oxidation during the temperature drop is kinetically limited and remains the excess of oxidizing factor (Gale, 2015; Macherzynski, 2018, Section 2). SCR catalysts change Hg speciation by converting a part of Hg(0) to Hg^{2+}. High quantities of Hg^{2+}, if obtained inside the SCR catalysts, can be removed inside downstream devices, such as ESP (in dust bonded form) and WFGD. ESP is highly efficient in Hg_p capture. Particulate matter removal inside ESPs is influenced by flue gas temperature, Hg^{2+} concentration, fly ash components, and other factors. Due to the high water solubility of Hg^{2+}, WFGDs have high co-removal performance, capturing between 48% and 98% of mercury (Table 4). However, Hg(0) reemission may occur during desulphurization process, which is influenced by operating temperature, pH, O_2 concentration in the flue gas, and the concentration of transition metal ions. The total mercury reduction rate in process gases treated with SCR + ESP + WFGD was around 36.5–94.4%, and for SCR + ESP + WFGD + WESP was reported at levels of 56.59–89.07% (Table 4, Table 5).
4. Hg removal efficiencies are generally lower in metallurgical plants and cement plants than in CFPPs. Instead of SCR systems, LNB systems are used in metallurgical plants to remove NO_x from exhaust gas, as in cement plants PM recycling systems are used. Mercury is returned to the kiln as a part of the PM, and the kiln system is enriched with mercury. It causes more Hg(0) to break through the PCD. In turn, MSWIPs exhibit a wide range of mercury removal efficiency: 33.6–96.2%.
5. Numerous reactions have been proposed to describe Hg(0) speciation changes in process gases, including homogenous and heterogeneous reactions. In homogenous reactions, halogen species oxidize Hg(0) at an optimum temperature of over 400 °C (Senior et al., 2000a). However, in heterogeneous reactions, fly ash or UBC promotes the oxidation of Hg(0) by halogen species when the process gas has the same concentration of halogen species as in the homogenous reactions. The four main heterogeneous reaction mechanisms: Deacon, Eley–Rideal, Langmuir–Hinshelwood, and the Mars–Maessen, were described in Section 3.
6. Sulfur compounds have strong effects on Hg(0) oxidation mechanisms in process gases. H_2S is a pollutant present in coal-derived or biomass-derived syngas. The metal oxides or carbon based metal oxide materials are a good option for removing both H_2S and Hg(0) from process gas. Metal-impregnate, metal sulfide materials and/or gaseous H_2S interact with mercury in process gases to form HgS. SO_2 usually inhibits the catalytical promotion of Hg(0) oxidation in exhaust gas. When metal sulfides were applied as sorbents, SO_2 had no significant effect on Hg(0) capture (Liu et al., 2019). The industrial im-

Table 5. Comparison of mercury capture effectiveness with different APCDs methods in various industries.

Sources of mercury emission	Air pollutant controlling methods	Total mercury capture effectiveness and reference(s)
CFPPs	ESP+FGD	44.5–98.53% (X. Li et al., 2019; Liu et al., 2019; Pilar et al., 2021)
	SCR+ESP+WFGD	63.54–74.11% (Su et al., 2017) 85.3% (Wang, 2020a) 36.5–94.4% (Table 4)
	SCR+ESP+WFGD+WESP	56.59–89.07% (Zhao et al., 2019a)
Iron metal plants	ESP+WFGD	80.6–86% (Fukuda et al., 2011) 24–85% (Wang et al., 2016)
	ESP+WFGD+PCDD/F	80–95% (Remus et al., 2013)
Industrial waste	WS + WESP	92.7% (Takahashi et al., 2012)
	DS or SDS + FF	96.3–98.7% (Park et al., 2008)
MSW	Spray absorber+FF or Spray dry absorber+FF+SCR	85.54–86.96% (Park et al., 2008)
	FBA+WS	96.2%
	ESP+FBA	95.6% (Hu et al., 2018)
	ESP+FF+WS+DSI	94.9%
Cement plants	ESP+FF	> 70% (Wang et al., 2014)
	ESP	64–90.2% (Chou et al., 2018)
	FF	95–98% (Mlakar et al., 2010)
	DS or SDS	80–90% (Mohee, 2013)
	ACI	> 75%

plementation of SRB biotechnique may be the next generation technology for Hg(0) removal in process gases, but more studies have to be performed to investigate its role and activity in heavy metal fixation as well as possible contribution to steel structure corrosion and coproduction of organometallics (Brown et al., 2012; Hsu-Kim et al., 2013).

ACKNOWLEDGEMENTS

The work was supported by the AGH University of Science and Technology with grant no. 16.16.210.476 B02.

REFERENCES

Abad-Valle P., Lopez-Anton M.A., Diaz-Somoano M., Martinez-Tarazona M.R., 2011. The role of unburned carbon concentrates from fly ashes in the oxidation and retention of mercury. *Chem. Eng. J.*, 174(1), 86–92. DOI: 10.1016/j.cej.2011.08.053.

Ahmaruzzaman M., 2010. A review on the utilization of fly ash. *Prog. Energy Combust. Sci.*, 36, 327–363. DOI: 10.1016/j.pecs.2009.11.003.

Altaf A.R., Adewuyi Y.G., Teng H., Gang L., Abid F., 2022. Elemental mercury (Hg^0) removal from coal syngas using magnetic tea-biochar: Experimental and theoretical insights. *J. Environ. Sci.*, 122, 150–161. DOI: 10.1016/J.JES.2021.09.033.

An M., Guo Q., Wei X., 2023. Reaction mechanism of H_2S with Hg^0 on $CuFe_2O_4$ oxygen carrier with oxygen vacancy structure during coal chemical looping gasification. *Fuel*, 333, Part 2, 126477. DOI: 10.1016/j.fuel.2022.126477.

ASTM, 2010. ASTM C618-23e1: Standard specification for coal fly ash and raw or calcined natural pozzolan for use in concrete. *Annual Book of ASTM Standards*, *C*, 3–6. DOI: 10.1520/C0618.

Auguścik-Górajek J., Nieć M., 2020. The variability of mercury content in bituminous coal seams in the coal basins in Poland. *Resources*, 9, 127. DOI: 10.3390/resources9110127.

Becker C., 2018. *From Langmuir to Ertl: The "Nobel" history of the surface science approach to heterogeneous catalysis. Encyclopedia of Interfacial Chemistry*, 99–106. DOI: https://doi.org/10.1016/B978-0-12-409547-2.13527-9

Białecka B., Pyka I., 2016. *Rtęć w polskim węglu kamiennym do celów energetycznych i w produktach jego przeróbki*. Główny Instytut Górnictwa, Katowice. Available at: https://gig.eu/sites/default/files/attachments/publikacje/monografia_19_05_2016.pdf.

Brown B.P., Brown S.R., Senko J.M., Dillon J., Spear J.R., Magnuson T., Building F., 2012. Microbial communities associated with wet flue gas desulfurization systems. *Front. Microbiol.*, 3. DOI: 10.3389/fmicb.2012.00412.

Cao Q., Qian Y., Liang H., Li Z., Chen S., Yang L., Zhan Q., 2020a. Mercury forms and their transformation in pyrite under weathering. *Surf. Interface Anal.*, 52, 283–292. DOI: 10.1002/sia.6718.

Cao Q., Yang L., Qian Y., Liang H., 2020b. Study on mercury species in coal and pyrolysis-based mercury removal before utilization. *ACS Omega*, 5, 20215-20223. DOI: 10.1021/acsomega.0c01875.

Cao Y., Duan Y., Kellie S., Li L., Xu W., Riley J.T., Pan W.P., Chu P., Mehta A.K., Carty R., 2005. Impact of coal chlorine on mercury speciation and emission from a 100-MW utility boiler with cold-side electrostatic precipitators and low-NO_x burners. *Energy Fuels*, 19, 842–854. DOI: 10.1021/ef034107u.

Caravati E.M., Erdman A.R., Christianson G., Nelson L.S., Woolf A.D., Booze L.L., Cobaugh D.J., Chyka P.A., Scharman E.J., Manoguerra A.S., Troutman W.G., 2008. Elemental mercury exposure: An evidence-based consensus guideline for out-of-hospital management. *Clin. Toxicol.*, 46, 1–21. DOI: 10.1080/15563650701664731.

Cha I.T., Roh S.W., Kim S.J., Hong H.J., Lee H.W., Lim W.T., Rhee S.K., 2013. Desulfotomaculum tongense sp. nov., a moderately thermophilic sulfate-reducing bacterium isolated from a hydrothermal vent sediment collected from the Tofua Arc in the Tonga Trench. *Antonie van Leeuwenhoek*, 104, 1185–1192. DOI: 10.1007/s10482-013-0040-0.

Chang L., Zhao Y., Li H., Tian C., Zhang Y., Yu X., Zhang J., 2017. Effect of sulfite on divalent mercury reduction and re-emission in a simulated desulfurization aqueous solution. *Fuel Process. Technol.*, 165, 138–144. DOI: 10.1016/j.fuproc.2017.05.016.

Chen C., Liu S., Gao Y., Liu Y., 2014. Investigation on mercury reemission from limestone-gypsum wet flue gas desulfurization slurry. *Sci. World J.*, 2014, 581724. DOI: 10.1155/2014/581724.

Chen Z., Mannava D.P., Mathur V.K., 2006. Mercury oxidization in dielectric barrier discharge plasma system. *Ind. Eng. Chem. Res.*, 45, 6050–6055. DOI: 10.1021/ie0603666.

Chou C.P., Chang T.C., Chiu C.H., Hsi H.C., 2018. Mercury speciation and mass distribution of cement production process in Taiwan. *Aerosol Air Qual. Res.*, 18, 2801–2812. DOI: 10.4209/aaqr.2018.05.0205.

Chou C.-P., Chiu C.-H., Chang T.C., Hsi H.C., 2021. Mercury speciation and mass distribution of coal-fired power plants in Taiwan using different air pollution control processes. *J. Air Waste Manage. Assoc.*, 71, 553–563. DOI: 10.1080/10962247.2020.1860158.

Deng Y., Macherzyński M., 2022. The influence of contact time between Hg reach flue gas and sorbents on Hg(0) capture in two kinds of laboratory reactor. *ICMGP 2022: 15th International Conference on Mercury as a Global Pollutant*. 24th–29th July 2022. ID 36, 1–20.

Dranga B.A., Lazar L., Koeser H., 2012. Oxidation catalysts for elemental mercury in flue gases – A review. *Catalysts*, 2, 139–170. DOI: 10.3390/catal2010139.

Du W., Yin L., Zhuo Y., Xu Q., Zhang L., Chen C., 2014. Catalytic oxidation and adsorption of elemental mercury over $CuCl_2$-impregnated sorbents. *Ind. Eng. Chem. Res.*, 53, 582–591. DOI: 10.1021/ie4016073.

Dziok T., Kołodziejska E.K., Kołodziejska E.L., 2020. Mercury content in woody biomass and its removal in the torrefaction process. *Biomass Bioenergy*, 143, 105832. DOI: 10.1016/j.biombioe.2020.105832.

Fan X., Li C., Zeng G., Zhang X., Tao S., Lu P., Tan Y., Luo D., 2012. Hg^0 removal from simulated flue gas over CeO_2/HZSM-5. *Energy Fuels*, *26*, 2082–2089. DOI: 10.1021/ef201739p.

Ferreira C.A., Ni D., Rosenkrans Z.T., Cai W., 2018. Scavenging of reactive oxygen and nitrogen species with nanomaterials. *Nano Res.*, 11, 4955–4984. DOI: 10.1007/s12274-018-2092-y.

Finkelman R.B., 1993. Trace and minor elements in coal. In: Engel M.H., Macko S.A. (Eds.), *Organic Geochemistry. Topics in Geobiology*. Springer, Boston, MA, 11, 593-607. DOI: 10.1007/978-1-4615-2890-6_28.

Finkelman R.B., Palmer C.A., Krasnow M.R., Aruscavage P.J., Sellers G.A., Dulong F.T., 1990. Combustion and leaching behavior of elements in the argonne premium coal samples. *Energy Fuels*, 4, 755–766. DOI: 10.1021/ef00024a024.

Font O., Córdoba P., Leiva C., Romeo L.M., Bolea I., Guedea I., Moreno N., Querol X., Fernandez C., Díez L.I., 2012. Fate and abatement of mercury and other trace elements in a coal fluidised bed oxy combustion pilot plant. *Fuel*, 95, 272–281. DOI: 10.1016/j.fuel.2011.12.017.

Fukuda N., Takaoka M., Doumoto S., Oshita K., Morisawa S., Mizuno T., 2011. Mercury emission and behavior in primary ferrous metal production. *Atmos. Environ.*, 45, 3685–3691. DOI: 10.1016/j.atmosenv.2011.04.038.

Galbreath K.C., Zygarlicke C.J., 2000. Mercury transformations in coal combustion flue gas. *Fuel Process. Technol.*, 65, 289–310. DOI: 10.1016/S0378-3820(99)00102-2.

Gale T.K., Lani B.W., Offen G.R., 2008. Mechanisms governing the fate of mercury in coal-fired power systems. *Fuel Process. Technol.*, 89, 139–151. DOI: 10.1016/j.fuproc.2007.08.004.

Gallego S., Benavides M., Tomaro M., 2002. Involvement of an antioxidant defence system in the adaptive response to heavy metal ions in *Helianthus annuus* L. cells. *Plant Growth Regul.*, 36, 267–273. DOI: 10.1023/A:1016536319908.

Gao Y., Zhang Z., Wu J., Duan L., Umar A., Sun L., Guo Z., Wang Q., 2013. A critical review on the heterogeneous catalytic oxidation of elemental mercury in flue gases. *Environ. Sci. Technol.*, 47, 10813–10823. DOI: 10.1021/es402495h.

Gibb W.H., Clarke F., Mehta A.K., 2000. The fate of coal mercury during combustion. *Fuel Process. Technol.*, 65, 365–377. DOI: 10.1016/S0378-3820(99)00104-6.

Gingerich D.B., Zhao Y., Mauter M.S., 2019. Environmentally significant shifts in trace element emissions from coal plants complying with the 1990 Clean Air Act Amendments. *Energy Policy*, 132, 1206–1215. DOI: 10.1016/J.ENPOL.2019.07.003.

Gołaś J., Strugała A., 2013. *Mercury as a coal combustion pollutant: monograph*. Oficyna Drukarska – Jacek Chmielewski, Warsaw, 97-99.

Gorecki J., Macherzynski M., Chmielowiec J., Borovec K., Wałeka M., Deng Y., Sarbinowski J., Pasciak G., 2022. The

methods and stands for testing fixed sorbent and sorbent polymer composite materials for the removal of mercury from flue gases. *Energies*, 15, 8891. DOI: 10.3390/en15238891.

Granite E.J., Pennline H.W., Hargis R.A., 2000. Novel sorbents for mercury removal from flue gas. *Ind. Eng. Chem. Res.*, 39, 1020–1029. DOI: 10.1021/ie990758v.

Hall B., Schager P., Lindqvist O., 1991. Chemical reactions of mercury in combustion flue gases. *Water Air Soil Pollut.*, 56, 3–14. DOI: 10.1007/BF00342256.

He Z., Xie Y., Wang Y., Xu J., Hu J., 2020. Removal of mercury from coal-fired flue gas and its sulfur tolerance characteristics by Mn, Ce modified γ-Al_2O_3 catalyst. *J. Chem.*, 2020, 8702745. DOI: 10.1155/2020/8702745.

Hower J.C., Senior C.L., Suuberg E.M., Hurt R.H., Wilcox J.L., Olson E.S., 2010. Mercury capture by native fly ash carbons in coal-fired power plants. *Prog. Energy Combust. Sci.*, 36, 510–529. DOI: 10.1016/j.pecs.2009.12.003.

Hisham M.W.M., Benson S.W., 1995. Thermochemistry of the deacon process. *J. Phys. Chem.*, 99, 6194–6198. DOI: 10.1021/j100016a065.

Hrdlicka J.A., Seames W.S., Mann M.D., Muggli D.S., Horabik C.A., 2008. Mercury oxidation in flue gas using gold and palladium catalysts on fabric filters. *Environ. Sci. Technol.*, 42, 6677–6682. DOI: 10.1021/es8001844.

Hsu-Kim H., Kucharzyk K.H., Zhang T., Deshusses M.A., 2013. Mechanisms regulating mercury bioavailability for methylating microorganisms in the aquatic environment: A critical review. *Environ. Sci. Technol.*, 47, 2441–2456. DOI: 10.1021/es304370g.

Hu Y., Cheng H., Tao S., 2018. The growing importance of waste-to-energy (WTE) incineration in China's anthropogenic mercury emissions: Emission inventories and reduction strategies. *Renewable Sustainable Energy Rev.*, 97, 119–137. DOI: 10.1016/j.rser.2018.08.026.

Huang Y., Liu J., Wang G., Wang Q., Zeng B., Xiao Z., Sun G., Li Z., 2022. Leachability of mercury in coal fly ash from coal-fired power plants in southwest China. *Front. Environ. Sci.*, 10, 887837. DOI: 10.3389/fenvs.2022.887837.

Huang Z., Wei Z., Xiao X., Tang M., Li B., Ming S., Cheng X., 2019. Bio-oxidation of Elemental Mercury into Mercury Sulfide and Humic Acid-Bound Mercury by Sulfate Reduction for Hg0 Removal in Flue Gas. *Environ. Sci. Technol.*, 53, 12923–12934. DOI: 10.1021/acs.est.9b04029.

Kern S., Salzer F., Reinhold H., 2015. Breaking the mercury cycle for emission abatement with the "ExMercury – Splitted Preheater System". *ZKG Cement Lime Gypsum* 9, 38–44.

Kho F., Koppel D.J., von Hellfeld R., Hastings A., Gissi F., Cresswell T., Higgins S., 2022. Current understanding of the ecological risk of mercury from subsea oil and gas infrastructure to marine ecosystems. *J. Hazard. Mater.*, 438, 129348. DOI: 10.1016/j.jhazmat.2022.129348.

Kolker A., Senior C.L., Quick J.C., 2006. Mercury in coal and the impact of coal quality on mercury emissions from combustion systems. *Appl. Geochem.*, 21, 1821–1836. DOI: 10.1016/j.apgeochem.2006.08.001.

Krukenberg V., Harding K., Richter M., Glöckner F.O., Gruber-Vodicka H.R., Adam B., Berg J.S., Knittel K., Tegetmeyer H.E., Boetius A., Wegener G., 2016. *Candidatus* Desulfofervidus auxilii, a hydrogenotrophic sulfate-reducing bacterium involved in the thermophilic anaerobic oxidation of methane. *Environ. Microbiol.*, 18, 3073–3091. DOI: 10.1111/1462-2920.13283.

Laudal D.L., Thompson J.S., Pavlish J.H., Chu P., Srivastava R.K., Lee C.W., Kilgroe J.D., 2002. Evaluation of mercury speciation at power plants using SCR and SNCR control technologies. *International Air Quality Conference III*, Arlington, VA, 9–12 September 2002.

Lee C. W., Serre S. D., Zhao Y., Hastings T.W., 2006. Study of the effect of chlorine addition on mercury oxidation by SCR catalyst under simulated subbituminous coal flue gas. *Proceedings, EPA-DOE-EPRI-A&WMA Power Plant Air Pollutant Control "Mega" Symposium*, Baltimore, MD, 28–31 August 2006. AWMA, Pittsburgh, PA, 13.

Li B., Wang H., 2021. Effect of flue gas purification facilities of coal-fired power plant on mercury emission. *Energy Rep.*, 7, 190–196. DOI: 10.1016/j.egyr.2021.01.094.

Li G., Shen B., Li Y., Zhao B., Wang F., He C., Wang Y., Zhang M., 2015. Removal of element mercury by medicine residue derived biochars in presence of various gas compositions. *J. Hazard. Mater.*, 298, 162–169. DOI: 10.1016/j.jhazmat.2015. 05.031.

Li G., Wu Q., Wang S., Duan Z., Su H., Zhang L., Li Z., Tang Y., Zhao M., Chen L., Liu K., Zhang Y., 2018. Improving flue gas mercury removal in waste incinerators by optimization of carbon injection rate. *Environ. Sci. Technol.*, 52, 1940–1945. DOI: 10.1021/acs.est.7b05560.

Li G., Wu Q., Wang S., Li Z., Liang H., Tang Y., Zhao M., Chen L., Liu K., Wang F., 2017. The influence of flue gas components and activated carbon injection on mercury capture of municipal solid waste incineration in China. *Chem. Eng. J.*, 326, 561–569. DOI: 10.1016/j.cej.2017.05.099.

Li X., Li Z., Fu C., Tang L., Chen J., Wu T., Lin C.J., Feng X., Fu X., 2019. Fate of mercury in two CFB utility boilers with different fueled coals and air pollution control devices. *Fuel*, 251, 651–659. DOI: 10.1016/j.fuel.2019.04.071.

Li Y., Yang D., Zhou X., Dong L., Sou L., Sun W., 2022a. Heavy metal migration characteristics of co-combustion between sewage sludge and high alkaline coal on circulating fluidized bed. *J. Therm. Sci.*, 31, 2178–2188. DOI: 10.1007/s11630-022-1695-5.

Li Z., Huang Y., Li X., Wang G., Wang Q., Sun G., Feng X., 2022b. Substance Flow Analysis of Zinc in Two Preheater-Precalciner Cement Plants and the Associated Atmospheric Emissions. *Atmosphere*, 13, 128. DOI: 10.3390/atmos13010128.

Ling L., Fan M., Wang B., Zhang R., 2015. Application of computational chemistry in understanding the mechanisms of mercury removal technologies: A review. *Energy Environ. Sci.*, 8, 3109–3133. DOI: 10.1039/c5ee02255j.

Liu D., Zhang Z., Wu J., Li C., 2020. Copper sulfide microsphere for Hg^0 capture from flue gas at low temperature. *Mater. Today Commun.*, *25*, 101188. DOI: 10.1016/j.mtcomm.2020.101188.

Liu S., Chen J., Cao Y., Yang H., Chen C., Jia W., 2019. Distribution of mercury in the combustion products from coal-fired power plants in Guizhou, southwest China. *J. Air Waste Manage. Assoc.*, 69, 234–245. DOI: 10.1080/10962247.2018.1535461.

Liu S., Liu W., Jiao F., Qin W., Yang C., 2021. Production and resource utilization of flue gas desulfurized gypsum in China – A review. *Environ. Pollut.*, 288, 117799. DOI: 10.1016/j.envpol.2021.117799.

Liu X., Wang S., Zhang L., Wu Y., Duan L., Hao J., 2013. Speciation of mercury in FGD gypsum and mercury emission during the wallboard production in China. *Fuel*, 111, 621–627. DOI: 10.1016/j.fuel.2013.03.052.

Luo G., Yao H., Xu M., Gupta R., Xu Z., 2011. Identifying modes of occurrence of mercury in coal by temperature programmed pyrolysis. *Proc. Combust. Inst.*, 33, 2763–2769. DOI: 10.1016/j.proci.2010.06.108.

Luo Z., Hu C., Zhou J., Cen K., 2006. Stability of mercury on three activated carbon sorbents. *Fuel Process. Technol.*, 87, 679–685. DOI: 10.1016/j.fuproc.2005.10.005.

Macherzynski M., 2018. *Reduction of mercury emission to the environment – selected problems and examples of laboratory and industrial tests*. ydawnictwa AGH, 60–62.

Maiti D., Ansari I., Rather M.A., Deepa A., 2019. Comprehensive review on wastewater discharged from the coal-related industries – characteristics and treatment strategies. *Water Sci. Technol.*, 79, 2023–2035. DOI: 10.2166/wst.2019.195.

Marcantonio V., Bocci E., Ouweltjes J.P., del Zotto L., Monarca D., 2020. Evaluation of sorbents for high temperature removal of tars, hydrogen sulphide, hydrogen chloride and ammonia from biomass-derived syngas by using Aspen Plus. *Int. J. Hydrogen Energy*, 45, 6651–6662. DOI: 10.1016/j.ijhydene.2019.12.142.

Martin G., Sharma S., Ryan W., Srinivasan N.K., Senko J.M., 2021. Identification of microbiological activities in wet flue gas desulfurization systems. *Front. Microbiol.*, 12, 675628. DOI: 10.3389/fmicb.2021.675628.

Masoomi I., Kamata H., Yukimura A., Ohtsubo K., Schmid M.O., Scheffknecht G., 2020. Investigation on the behavior of mercury across the flue gas treatment of coal combustion power plants using a lab-scale firing system. *Fuel Process. Technol.*, 201, 106340. DOI: 10.1016/j.fuproc.2020.106340.

Mathebula M.W., Panichev N., Mandiwana K., 2020. Determination of mercury thermospecies in South African coals in the enhancement of mercury removal by pre-combustion technologies. *Sci. Rep.*, 10, 19282. DOI: 10.1038/s41598-020-76453-z.

Merdes A.C., Keener T.C., Khang S.J., Jenkins R.G., 1998. Investigation into the fate of mercury in bituminous coal during mild pyrolysis. *Fuel*, 77, 1783–1792. DOI: 10.1016/S0016-2361(98)00087-8.

Michalska A., Smolinski A., Koteras A., 2022. Analysis of mercury content inside mining waste dump case study in the Upper Silesia in Poland. *Arch. Min. Sci.*, 67, 95–106. DOI: 10.24425/ams.2022.140704.

Mlakar T.L., Horvat M., Vuk T., Stergaršek A., Kotnik J., Tratnik J., Fajon V., 2010. Mercury species, mass flows and processes in a cement plant. *Fuel*, 89, 1936–1945. DOI: 10.1016/j.fuel.2010.01.009.

Mohee F., 2013. A review of the effects and control of the mercury emissions from cement industry. *EIC – Climate Change Technology Conference 2013*. Montreal, Canada, May 2013.

Mojammal A.H.M., Back S.K., Seo Y.C., Kim J.H., 2019. Mass balance and behavior of mercury in oil refinery facilities. *Atmos. Pollut. Res.*, 10, 145–151. DOI: 10.1016/j.apr.2018.07.002.

Mukherjee A.B., Zevenhoven R., Bhattacharya P., Sajwan K.S., Kikuchi R., 2008. Mercury flow via coal and coal utilization by-products: A global perspective. *Resour. Conserv. Recycl.*, 52, 571–591. DOI: 10.1016/j.resconrec.2007.09.002.

Neveux T., Hagi H., le Moullec Y., 2014. Performance simulation of full-scale wet flue gas desulfurization for oxy-coal combustion. *Energy Procedia*, 63, 463–470. DOI: 10.1016/j.egypro.2014.11.049.

Niu Q., Luo J., Sun S., Chen Q., Lu J., 2015. Effects of flue gas components on the oxidation of gaseous Hg^0 by dielectric barrier discharge plasma. *Fuel*, 150, 619–624. DOI: 10.1016/j.fuel.2015.02.043.

Okonji S.O., Achari G., Pernitsky D., 2021. Environmental impacts of selenium contamination: A review on current-issues and remediation strategies in an aqueous system. *Water*, 13, 1473. DOI: 10.3390/w13111473.

Okońska A., Uruski Ł., Górecki J., Gołaś J., 2013. Metodyka oznaczania zawartości rtęci całkowitej w węglach energetycznych. *Gospodarka Surowcami Mineralnymi*, 29, 39–49. DOI: 10.2478/gospo-2013-0019.

Omine N., Romero C.E., Kikkawa H., Wu S., Eswaran S., 2012. Study of elemental mercury re-emission in a simulated wet scrubber. *Fuel*, 91, 93–101. DOI: 10.1016/j.fuel.2011.06.018.

Osipova N.A., Tkacheva E.V., Arbuzov S.I., Yazikov E.G., Matveenko I.A., 2019. Mercury in coals and soils from coal-mining regions. *Solid Fuel Chem.*, 53, 411–417. DOI: 10.3103/S036152191907005X.

Park K.S., Seo Y.C., Lee S.J., Lee J.H., 2008. Emission and speciation of mercury from various combustion sources. *Powder Technol.*, 180, 151–156. DOI: 10.1016/j.powtec.2007.03.006.

Pavlish J.H., Sondreal E.A., Mann M.D., Olson E.S., Galbreath K.C., Laudal D.L., Benson S.A., 2003. Status review of mercury control options for coal-fired power plants. *Fuel Process. Technol.,* 82,89-165. DOI: 10.1016/S0378-3820(03)00059-6.

Pilar L., Borovec K., Szeliga Z., Górecki J., 2021. Mercury emission from three lignite-fired power plants in the Czech Republic. *Fuel Process. Technol.*, 212, 106628. DOI: 10.1016/j.fuproc.2020.106628.

Presto A.A., Granite E.J., 2008. Noble metal catalysts for mercury oxidation in utility flue gas. *Platinum Met. Rev.*, 52, 144–154. DOI: 10.1595/147106708X319256.

Prins R., 2018. Eley–Rideal, the other mechanism. *Top. Catal.*, 61, 714–721. DOI: 10.1007/s11244-018-0948-8.

Puig-Arnavat M., Bruno J.C., Coronas A., 2010. Review and analysis of biomass gasification models. *Renewable Sustainable Energy Rev.*, 14, 2841–2851. DOI: 10.1016/j.rser.2010.07.030.

Qiao Y., Xu M., Yao H., Wang C., Gong X., Chen H., Li L., 2007. Modeling of homogeneous tin speciation using detailed chemical kinetics. *Asia-Pac. J. Chem. Eng.*, 2, 158–164. DOI: 10.1002/apj.35.

Rahim D.A., Fang W., Wibowo H., Hantoko D., Susanto H., Yoshikawa K., Zhong Y., Yan M., 2023. Review of high temperature H_2S removal from syngas: Perspectives on downstream process integration. *Chem. Eng. Process. Process Intensif.*, 183, 109258. DOI: 10.1016/j.cep.2022.109258.

Raj D., Chowdhury A., Maiti S.K., 2017. Ecological risk assessment of mercury and other heavy metals in soils of coal mining area: A case study from the eastern part of a Jharia coal field, India. *Hum. Ecol. Risk Assess.: Int. J.*, 23, 767–787. DOI: 10.1080/10807039.2016.1278519.

Remus R., Aguado-Monsonet M.A., Roudier S., Delgado Sancho L., 2013. *Best available techniques (BAT) reference document for iron and steel production. Industrial emissions Directive 2010/75/EU: integrated pollution prevention and control*. Joint Research Centre, Institute for Prospective Technological Studies, Publications Office. https://data.europa.eu/doi/10.2791/97469.

Ren W., Yang L., Cao Q., Liang C., 2021. Concentration, distribution and occurrence of mercury in Chinese coals. *E3S Web Conf.*, 290, 03003. DOI: 10.1051/e3sconf/202129003003.

Rumayor M., Lopez-Anton M.A., Díaz-Somoano M., Martínez-Tarazona M.R., 2015. A new approach to mercury speciation in solids using a thermal desorption technique. *Fuel*, 160, 525–530. DOI: 10.1016/j.fuel.2015.08.028.

Schneider L., Rose N.L., Myllyvirta L., Haberle S., Lintern A., Yuan J., Sinclair D., Holley C., Zawadzki A., Sun R., 2021. Mercury atmospheric emission, deposition and isotopic fingerprinting from major coal-fired power plants in Australia: Insights from palaeo-environmental analysis from sediment cores. *Environ. Pollut.*, 287, 117596. DOI: 10.1016/j.envpol.2021.117596.

Senior C.L., Sarofim A.F., Zeng T., Helble J.J., Mamani-Paco R., 2000a. Gas-phase transformations of mercury in coal-fired power plants. *Fuel Process. Technol.*, 63, 197–213. DOI: 10.1016/S0378-3820(99)00097-1 .

Senior C., Linjewile T., 2003. *Oxidation of mercury across SCR catalysts in coal-fired power plants burning low rank fuels*. United Sates. DOI: 10.2172/822762.

Senior C., Granite E., Linak W., Seames W., 2020b. Chemistry of Trace inorganic elements in coal combustion systems: a century of discovery. *Energy Fuels*, 34, 15141–15168. DOI: 10.1021/acs. energyfuels.0c02375.

Sliger R.N., Kramlich J.C., Marinov N.M., 2000. Towards the development of a chemical kinetic model for the homogeneous oxidation of mercury by chlorine species. *Fuel Process. Technol.*, 65-66, 423–438. DOI: 10.1016/S0378-3820(99)00108-3.

Srivastava R.K., Hutson N., Martin B., Princiotta F., Staudt J., 2006. Control of mercury emissions from coal-fired electric utility boilers. *Environ. Sci. Technol.*, 40, 1385–1393. DOI: 10.1021/es062639u.

Stolle R., Koeser H., Gutberlet H., 2014. Oxidation and reduction of mercury by SCR DeNO$_x$ catalysts under flue gas conditions in coal fired power plants. *Appl. Catal., B*, 144, 486–497. DOI: 10.1016/j.apcatb.2013.07.040.

Su S., Liu L., Wang L., Syed-Hassan S.S.A., Kong F., Hu S., Wang Y., Jiang L., Xu K., Zhang A., Xiang J., 2017. Mass flow analysis of mercury transformation and effect of seawater flue gas desulfurization on mercury removal in a full-scale coal-fired power plant. *Energy Fuels*, 31, 11109–11116. DOI: 10.1021/acs.energyfuels.7b02029.

Su Y., Liu X., Teng Y., Zhang K., 2021. Mercury speciation in various coals based on sequential chemical extraction and thermal analysis methods. *Energies*, 14, 2361. DOI: 10.3390/en14092361.

Sui Z., Zhang Y., Li W., Orndorff W., Cao Y., Pan W.-P., 2015. Partitioning effect of mercury content and speciation in gypsum slurry as a function of time. *J. Therm. Anal. Calorim.*, 119, 1611–1618. DOI: 10.1007/s10973-015-4403-9.

Sultanguzin I.A., Fedyukhin A.V., Zakharenkov E.A., Yavorovsky Y.V., Voloshenko E.V., Kurzanov S.Y., Stepanova T.A., Tumanovsky V.A., Ippolitov V.A., 2020. An Analysis of the prospects for coal-fired thermal power station reconstruction on the basis of coal gasification and a combined-cycle unit. *Therm. Eng.*, 67, 451–460. DOI: 10.1134/S004060152007006X.

Takahashi F., Shimaoka T., Kida A., 2012. Atmospheric mercury emissions from waste combustions measured by continuous monitoring devices. *J. Air Waste Manage. Assoc.*, 62, 686–695. DOI: 10.1080/10962247.2012.659329.

Tang K., Baskaran V., Nemati M., 2009. Bacteria of the sulphur cycle: An overview of microbiology, biokinetics and their role in petroleum and mining industries. *Biochem. Eng. J.*, 44, 73–94. DOI: 10.1016/j.bej.2008.12.011.

UN Environment, 2019. Global mercury assessment 2018. UN Environment Programme, Chemicals and Health Branch Geneva, Switzerland.

Uruski L., Gorecki J., Macherzynski M., Dziok T., Golas J., 2015. The ability of Polish coals to release mercury in the process of thermal treatment. *Fuel Process. Technol.*, 140, 12–20. DOI: 10.1016/j.fuproc.2015.08.005.

Villarini M., Marcantonio V., Colantoni A., Bocci E., 2019. Sensitivity analysis of different parameters on the performance of a CHP internal combustion engine system fed by a biomass waste gasifier. *Energies*, 12, 688. DOI: 10.3390/en12040688.

Wang F., Wang S., Zhang L., Yang H., Gao W., Wu Q., Hao J., 2016. Mercury mass flow in iron and steel production process and its implications for mercury emission control. *J. Environ. Sci.*, 43, 293–301. DOI: 10.1016/j.jes.2015.07.019.

Wang F., Wang S., Zhang L., Yang H., Wu Q., Hao J., 2014. Mercury enrichment and its effects on atmospheric emissions in cement plants of China. *Atmos. Environ.*, 92, 421–428. DOI: 10.1016/j.atmosenv.2014.04.029.

Wang J., Fang Y., Wang H., Bai G., Qin W., Zhang J., 2022. Simultaneous removal of Hg^0 and H_2S over a regenerable Fe_2O_3/AC catalyst. *Atmosphere*, 13, 425. DOI: 10.3390/atmos13030425.

Wang S., 2020a. Near-zero air pollutant emission technologies and applications for clean coal-fired power. *Engineering*, 6, 1408–1422. DOI: 10.1016/j.eng.2019.10.018.

Wang S.X., Zhang L., Li G.H., Wu Y., Hao J.M., Pirrone N., Sprovieri F., Ancora M.P., 2010a. Mercury emission and speci-

ation of coal-fired power plants in China. *Atmos. Chem. Phys.*, 10, 1183–1192. DOI: 10.5194/acp-10-1183-2010.

Wang Y., Duan Y., Yang L., Zhao C., Shen X., Zhang M., Zhuo Y., Chen C., 2009. Experimental study on mercury transformation and removal in coal-fired boiler flue gases. *Fuel Process. Technol.*, 90, 643–651. DOI: 10.1016/j.fuproc.2008.10.013.

Wang Z.H., Jiang S.D., Zhu Y.Q., Zhou J.S., Zhou J.H., Li Z.S., Cen K.F., 2010b. Investigation on elemental mercury oxidation mechanism by non-thermal plasma treatment. *Fuel Process. Technol.*, 91, 1395–1400. DOI: 10.1016/j.fuproc.2010.05.012.

Wang Z., Liu J., Yang Y., Miao S., Shen F., 2018. Effect of the mechanism of H_2S on elemental mercury removal using the MnO_2 sorbent during coal gasification. *Energy Fuels*, 32, 4453–4460. DOI: 10.1021/acs.energyfuels.7b03092.

Wang Z., Liu J., Yang Y., Yu Y., Yan X., Zhang Z., 2020b. AMn_2O_4 (A=Cu, Ni and Zn) sorbents coupling high adsorption and regeneration performance for elemental mercury removal from syngas. *J. Hazard. Mater.*, 388, 121738. DOI: 10.1016/j.jhazmat.2019.121738.

Wdowin M., Macherzyński M., Panek R., Górecki J., Franus W., 2015. Investigation of the sorption of mercury vapour from exhaust gas by an Ag-X zeolite. *Clay Miner.*, 50, 31–40. DOI: 10.1180/claymin.2015.050.1.04.

Wdowin M., Macherzyński M., Panek R., Wałęka M., Górecki J., 2020. Analysis of selected mineral and waste sorbents for the capture of elemental mercury from exhaust gases. *Mineralogia*, 51, 17–35. DOI: 10.2478/mipo-2020-0003

Wiatros-Motyka M.M., Sun C.G., Stevens L.A., Snape C.E., 2013. High capacity co-precipitated manganese oxides sorbents for oxidative mercury capture. *Fuel*, 109, 559–562. DOI: 10.1016/j.fuel.2013.03.019.

Wierzchowski K., Chećko J., Pyka I., 2017. Variability of mercury content in coal matter from coal seams of the upper Silesia coal basin. *Arch. Min. Sci.*, 62, 843–856. DOI: 10.1515/amsc-2017-0058.

Wu C.-L., Cao Y., He C.-C., Dong Z.-B., Pan W.-P., 2010. Study of elemental mercury re-emission through a lab-scale simulated scrubber. *Fuel*, 89, 2072–2080. DOI: 10.1016/j.fuel.2009.11.045.

Wu J., Cao Y., Pan W., Shen M., Ren J., Du Y., He P., Wang D., Xu J., Wu A., Li S., Lu P., Pan W.P., 2008. Evaluation of mercury sorbents in a lab-scale multiphase flow reactor, a pilot-scale slipstream reactor and full-scale power plant. *Chem. Eng. Sci.*, 63, 782–790. DOI: 10.1016/j.ces.2007.09.041.

Wu X., Duan Y., Meng J., Geng X., Shen A., Hu J., 2021. Experimental study on the mercury removal of a H_2S-modified Fe_2O_3 adsorbent. *Ind. Eng. Chem. Res.*, 60, 17429–17438. DOI: 10.1021/acs.iecr.1c01998.

Wu Y. W., Ali Z., Lu Q., Liu J., Xu M. X., Zhao L., Yang Y.P., 2019. Effect of WO_3 doping on the mechanism of mercury oxidation by HCl over V_2O_5/TiO_2 (001) surface: Periodic density functional theory study. *Appl. Surf. Sci.*, 487, 369–378. DOI: 10.1016/J.APSUSC.2019.05.132.

Xie Y., Li C., Zhao L., Zhang J., Zeng G., Zhang X., Zhang W., Tao S., 2015. Experimental study on Hg^0 removal from flue gas over columnar MnO_x-CeO_2/activated coke. *Appl. Surf. Sci.*, *333*, 59–67. DOI: 10.1016/j.apsusc.2015.01.234.

Xing X., Zhang X., Tang J., Cui L., Dong Y., 2022. Removal of gaseous elemental mercury from simulated syngas over Fe_2O_3/TiO_2 sorbents. *Fuel*, 311, 122614. DOI: 10.1016/j.fuel.2021.122614.

Xu J., Zhang A., Zhou Z., Wang C., Deng L., Liu L., Xia H., Xu M., 2021. Elemental mercury removal from flue gas over silver-loaded CuS-wrapped Fe_3O_4 sorbent. *Energy Fuels*, 35, 13975-13983. DOI: 10.1021/acs.energyfuels.1c02150

Xu Y.N., Chen Y., 2020. Advances in heavy metal removal by sulfate-reducing bacteria. *Water Sci. Technol.*, 81, 1797–1827. DOI: 10.2166/wst.2020.227.

Xue L., Liu T., Guo X., Zheng C., 2015. Hg oxidation reaction mechanism on Fe_2O_3 with H_2S: Comparison between theory and experiments. *Proc. Combust. Inst.*, 35, 2867–2874. DOI: 10.1016/j.proci.2014.06.065

Yan J., Yuan W., Liu J., Ye W., Lin J., Xie J., Huang X., Gao S., Xie J., Liu S., Chen W., Zhang H., 2019. An integrated process of chemical precipitation and sulfate reduction for treatment of flue gas desulphurization wastewater from coal-fired power plant. *J. Cleaner Prod.*, 228, 63–72. DOI: 10.1016/j.jclepro.2019.04.227.

Yang J., Li Q., Zhu W., Qu W., Li M., Xu Z., Yang Z., Liu H., Li H., 2021a. Recyclable chalcopyrite sorbent for mercury removal from coal combustion flue gas. *Fuel*, 290, 120049. DOI: 10.1016/j.fuel.2020.120049.

Yang Y., Liu J., Shen F., Zhao L., Wang Z., Long Y., 2016. Kinetic study of heterogeneous mercury oxidation by HCl on fly ash surface in coal-fired flue gas. *Combust. Flame*, 168, 1–9. DOI: 10.1016/j.combustflame.2016.03.022.

Yang Y., Liu J., Wang Z., Yu Y., 2021b. Reaction mechanism of elemental mercury oxidation to $HgSO_4$ during SO_2/SO_3 conversion over V_2O_5/TiO_2 catalyst. *Proc. Combust. Inst.*, 38, 4317–4325. DOI: 10.1016/j.proci.2020.10.007.

Yang Y., Zheng C., Su Q., Wang Y., Lu Y., Zhang Y., Zhu Y., 2021c. SOx removal and emission characteristics of WFGD system applied in ultra-low emission coal-fired power plants. *Case Stud. Therm. Eng.*, 28, 101562. DOI: 10.1016/j.csite.2021.101562.

Yue T., Wang F., Han B.J., Zuo P.L., Zhang F., 2013. Analysis on mercury emission and control technology of typical industries in China. *Appl. Mech. Mater.*, 295–298, 859–871. DOI: 10.4028/www.scientific.net/AMM.295-298.859.

Zhang A., Zheng W., Song J., Hu S., Liu Z., Xiang J., 2014. Cobalt manganese oxides modified titania catalysts for oxidation of elemental mercury at low flue gas temperature. *Chem. Eng. J.*, 236, 29–38. DOI: 10.1016/J.CEJ.2013.09.060.

Zhang J., Li L., Liu J., 2017a. Effects of irrigation and water content of packing materials on a thermophilic biofilter for SO_2 removal: Performance, oxygen distribution and microbial population. *Biochem. Eng. J.*, 118, 105–112. DOI: 10.1016/j.bej.2016.11.015.

Zhang L., Wang S., Wang L., Wu Y., Duan L., Wu Q., Wang F., Yang M., Yang H., Hao J., Liu X., 2015. Updated emission inventories for speciated atmospheric mercury from anthro-

pogenic sources in China. *Environ. Sci. Technol.*, 49, 3185–3194. DOI: 10.1021/es504840m.

Zhang L., Wang S., Wu Q., Wang F., Lin C.J., Zhang L., Hui M., Yang M., Su H., Hao J., 2016. Mercury transformation and speciation in flue gases from anthropogenic emission sources: a critical review. *Atmos. Chem. Phys.*, 16, 2417–2433. DOI: 10.5194/acp-16-2417-2016

Zhang Q., Mei J., Sun P., Zhao H., Guo Y., Yang S., 2020. Mechanism of elemental mercury oxidation over copper-based oxide catalysts: kinetics and transient reaction studies. *Ind. Eng. Chem. Res.*, 59, 61–70. DOI: 10.1021/acs.iecr.9b04806.

Zhang S., Díaz-Somoano M., Zhao Y., Yang J., Zhang J., 2019. Research on the mechanism of elemental mercury removal over Mn-based SCR catalysts by a developed Hg-TPD method. *Energy Fuels*, 33, 2467-2476. DOI: 10.1021/acs.energyfuels.8b04424.

Zhang Y., Yang J., Yu X., Sun P., Zhao Y., Zhang J., Chen G., Yao H., Zheng C., 2017b. Migration and emission characteristics of Hg in coal-fired power plant of China with ultra low emission air pollution control devices. *Fuel Process. Technol.*, 158, 272–280. DOI: 10.1016/j.fuproc.2017.01.020.

Zhao L., Li C., Zhang X., Zeng G., Zhang J., Xie Y., 2015. A review on oxidation of element mercury from coal-fired flue gas with selective catalytic reduction catalysts. *Catal. Sci. Technol.*, 5, 3459–3472. DOI: 10.1039/C5CY00219B.

Zhao S., Duan Y., Yao T., Liu M., Lu J., Tan H., Wang X., Wu L., 2017. Study on the mercury emission and transformation in an ultra-low emission coal-fired power plant. *Fuel*, 199, 653–661. DOI: 10.1016/j.fuel.2017.03.038.

Zhao S., Pudasainee D., Duan Y., Gupta R., Liu M., Lu J., 2019a. A review on mercury in coal combustion process: Content and occurrence forms in coal, transformation, sampling methods, emission and control technologies. *Prog. Energy Combust. Sci.*, 73, 26–64. DOI: 10.1016/j.pecs.2019.02.001.

Zhao S., Sun C., Zhang Y., Jiao T., Zhang W., Liang P., Zhang H., 2019b. Determination of mercury occurrence and thermal stability in high ash bituminous coal based on sink-float and sequential chemical extraction method. *Fuel*, 253, 571–579. DOI: 10.1016/j.fuel.2019.05.054.

Zheng S., Shi Y., Wang Z., Wang P., Liu G., Zhou H., 2021. Development of new technology for coal gasification purification and research on the formation mechanism of pollutants. *Int. J. Coal Sci. Technol.*, 8(3), 335–348. DOI: 10.1007/s40789-021-00420-w.

Zhou Q., Duan Y.F., Zhao S.L., Zhu C., She M., Zhang J., Wang S.Q., 2015a. Modeling and experimental studies of induct mercury capture by activated carbon injection in an entrained flow reactor. *Fuel Process. Technol.*, 140, 304–311. DOI: 10.1016/j.fuproc.2015.08.018.

Zhou Y., Yang J., Zhang Y., Zhang Y., Yu X., Zhao Y., Zhang J., Zheng C., 2019. Role of SO_3 in elemental mercury removal by magnetic biochar. *Energy Fuels*, 33, 11446–11453. DOI: 10.1021/acs.energyfuels.9b02567.

Zhou Z.J., Liu X.W., Zhao B., Chen Z.G., Shao H.Z., Wang L.L, Xu M.H., 2015b. Effects of existing energy saving and air pollution control devices on mercury removal in coal-fired power plants. *Fuel Process. Technol.*, 131, 99–108. DOI: 10.1016/j.fuproc.2014.11.014.

Zulaikhah S.T., Wahyuwibowo J., Pratama A.A., 2020. Mercury and its effect on human health: a review of the literature. *IJPHS*, 9, 103–114. DOI: 10.11591/ijphs.v9i2.20416.